

## Article

# Effectiveness of Protein and Polysaccharide Biopolymers as Dust Suppressants on Mine Soils: Large-Scale Field Trials

Johannes Lukas Sieger <sup>\*</sup>, Bernd Georg Lottermoser  and Justus Freer

Institute of Mineral Resources Engineering, RWTH Aachen University, 52062 Aachen, Germany

\* Correspondence: [sieger@mre.rwth-aachen.de](mailto:sieger@mre.rwth-aachen.de)

**Abstract:** Recent laboratory studies have shown that biopolymers have the potential to act as dust suppressants on barren mine soils. However, there is a lack of field trials investigating the effectiveness of biopolymer treatments under real field conditions on a large scale. This study performed field trials to examine the potential of three biopolymers—corn starch (CS), xanthan gum (XG), and fava bean protein concentrate (FBPC)—as dust suppressants. The field trials started in August 2022 with spraying of low doses of the selected biopolymers on trial areas of an overburden dump at the Inden open-cast lignite mine, Germany. The field trials were conducted over 45 days. They included repeated measurements of dust emissions from soil plots exposed to different airflows generated by an electric blower, visual inspections, and penetrometer tests. The results showed that all biopolymer treatments effectively suppressed dust emissions in the short term up to 8 days after application. Total suspended particle emissions measured on the biopolymer-treated trial plots were significantly reduced and ranged from 0.05 to 0.27 mg/m<sup>3</sup> compared to the untreated control (4.5 to 39.2 mg/m<sup>3</sup>). The visual inspections and penetrometer tests supported these results. After day 8, rainfall-induced leaching of the biopolymers resulted in the rapid degradation of the treatments' effectiveness. The results suggest that the treatments would have lasted longer under dry conditions. Thus, the field trials provide practical evidence that biopolymers can effectively mitigate dust emissions on exposed, undisturbed mine soils in the short term, making them a bio-based alternative to traditional dust suppressants, such as chloride salts or petroleum-based products.



**Citation:** Sieger, J.L.; Lottermoser, B.G.; Freer, J. Effectiveness of Protein and Polysaccharide Biopolymers as Dust Suppressants on Mine Soils: Large-Scale Field Trials. *Mining* **2023**, *3*, 428–462. <https://doi.org/10.3390/mining3030026>

Academic Editors: Mostafa Benzaazoua and Yassine Ait-khouia

Received: 12 June 2023  
Revised: 7 July 2023  
Accepted: 14 July 2023  
Published: 18 July 2023



**Copyright:** © 2023 by the authors. Licensee MDPI, Basel, Switzerland. This article is an open access article distributed under the terms and conditions of the Creative Commons Attribution (CC BY) license (<https://creativecommons.org/licenses/by/4.0/>).

**Keywords:** field trials; wind erosion; dust control; dust suppressant; mine soils; biopolymer; polysaccharide; protein; dust concentration; corn starch; fava bean protein; xanthan gum

## 1. Introduction

Dust emissions from active and abandoned mine sites have environmental, social, and economic impacts. They can affect local ecosystems [1,2], the health of workers and local communities [3–9], may pose safety risks due to reduced visibility [10,11], and can increase vehicle maintenance costs [11]. Furthermore, during strong wind events, dust can be transported and deposited on surrounding communities, causing a nuisance to residents. These mine dust emissions originate primarily from unpaved haul roads or large, exposed surfaces, such as tailings storage facilities, stockpiles, and overburden and waste dumps. They remain difficult to control due to their vast aerial extent and topographic exposition. During the operational phase of mines, revegetation of such areas is often not feasible from an operational perspective. The relevance of this issue will increase in the coming decades as both the extraction of raw materials and the frequency of droughts and strong wind events are predicted to increase [12–14].

The application of dust suppressants constitutes a proven method to mitigate emissions from exposed surfaces. However, many conventional dust suppressants, such as salt brines, petroleum-based products or synthetic polymers, are costly, can have adverse environmental effects [15], and the toxicity of (often proprietary) formulations is often insufficiently studied by independent third parties [16]. Furthermore, the ingredients of

most synthetic polymers are still predominantly produced by the petrochemical industry from fossil fuels (oil and natural gas) [17]. Therefore, in order to progress towards more sustainable raw material extraction, there is a need for dust suppressants that are bio-based, environmentally friendly, readily available, and cost-effective. To address this need, recent research has focused on investigating the potential of biopolymers as dust suppressants (e.g., [18–21]).

Biopolymers, such as starches and cellulose derivatives, are biodegradable and can be sourced from naturally abundant sources [22] or produced by microbial fermentation (e.g., xanthan gum) [23]. Dissolved in water, they can be sprayed on or mixed into the soil and act by agglomerating the soil particles, thereby increasing the wind erosion resistance of the soil. Recent laboratory studies have primarily analysed indicative parameters such as the penetration resistance [18–21,24,25], crust thickness [19,20,26,27], and moisture retention [21,27–31] of biopolymer-treated soil samples or measured the wind erosion resistance in wind tunnel studies [18,19,21,28,30,32–34]. While these laboratory studies have demonstrated the potential of biopolymers to act as dust suppressants, field trials are needed to investigate the effectiveness, durability, and scalability of their applications under actual field conditions. This need has recently also been articulated by Chang et al. [35] and Wade et al. [36].

In this study, large-scale field trials were conducted at the Inden open-cast lignite mine in Germany to evaluate the effectiveness of three selected biopolymers—corn starch (CS), fava bean concentrate (FBPC), and xanthan gum (XG)—in reducing dust emissions from exposed, undisturbed mine soils. The field trials build on two previous laboratory studies by Sieger et al. [37,38], which investigated the particle agglomeration potential and ability of selected biopolymers to enhance the soil wind erosion resistance. The field trials started with the large-scale application of biopolymers using a conventional field sprayer. Airflow-induced dust emissions were measured using a custom-built test setup and complemented by visual inspections of the plots tested and penetrometer testing. Acquired data were analysed in the context of meteorological data provided by a nearby weather station. Results of the presented field trials provide evidence that biopolymers can be used for effective short-term dust control on large, undisturbed mine soils.

## 2. Materials and Methods

### 2.1. Biopolymers

Previous studies by Sieger et al. [37] investigated the dust suppressant potential of 14 selected protein and polysaccharide biopolymers using penetrometer, moisture retention and crust thickness measurements. In a subsequent study, Sieger et al. [38] performed wind tunnel and penetrometer tests with 5 selected proteins and polysaccharides to investigate the wind erosion and penetration resistance of the biopolymer-treated soil samples at different application rates ( $L/m^2$ ) and concentrations (%). Based on the results of these studies, suitable application parameters (see Section 2.3) and three biopolymers were selected for this study:

*Corn starch (CS)*. Pre-gelatinised CS (type: CGel-Instant 12018) was obtained from Cargill B.V. (NL). According to the manufacturer's certificate of analysis, it has a moisture content of 5.8 wt%. The product primarily finds application as an instant thickener for puddings, sauces, soups, cakes, and bakery products.

*Xanthan gum (XG)*. Technical grade, readily dispersible XG (type: Xanthan TGRD) was obtained from Jungbunzlauer Austria AG (AT). It is a white, free-flowing powder, and according to the manufacturer's certificate of analysis, has a moisture content of 5.1 wt%.

*Fava bean protein concentrate (FBPC)*. Organic fava bean protein concentrate (60% protein content) was obtained from Aljoa-Starkelsen (LV). It comes as a creamy light-yellowish powder and has a moisture content of 8.8 wt%.

## 2.2. Field Trial Location and Mine Soil

The field trials were performed on the upper bench of the overburden dump of the Inden open-cast lignite mine in North Rhine-Westphalia, 40 km west of Cologne, Germany (Figure 1a). Four trial areas were prepared, one for each biopolymer tested (CS, XG, and FBPC) and an untreated control (C) (Figure 1b). Each trial area measured  $15 \times 100 \text{ m}^2$  and was marked with wooden stakes and flagging tape.

The particle size distribution was established for each trial area according to DIN EN ISO 17892-4 [39] (Figure 2 and Table 1) at the Unit of Mineral Processing, RWTH Aachen University. Each trial area was sampled at three locations, and samples were blended into representative composites. Based on the unified soil classification system (USCS), the material can be classified as medium- to fine-grained, poorly-graded sand (SP). All trial areas display similar particle size distributions, with the XG-treated area having a slightly coarser grain size distribution.

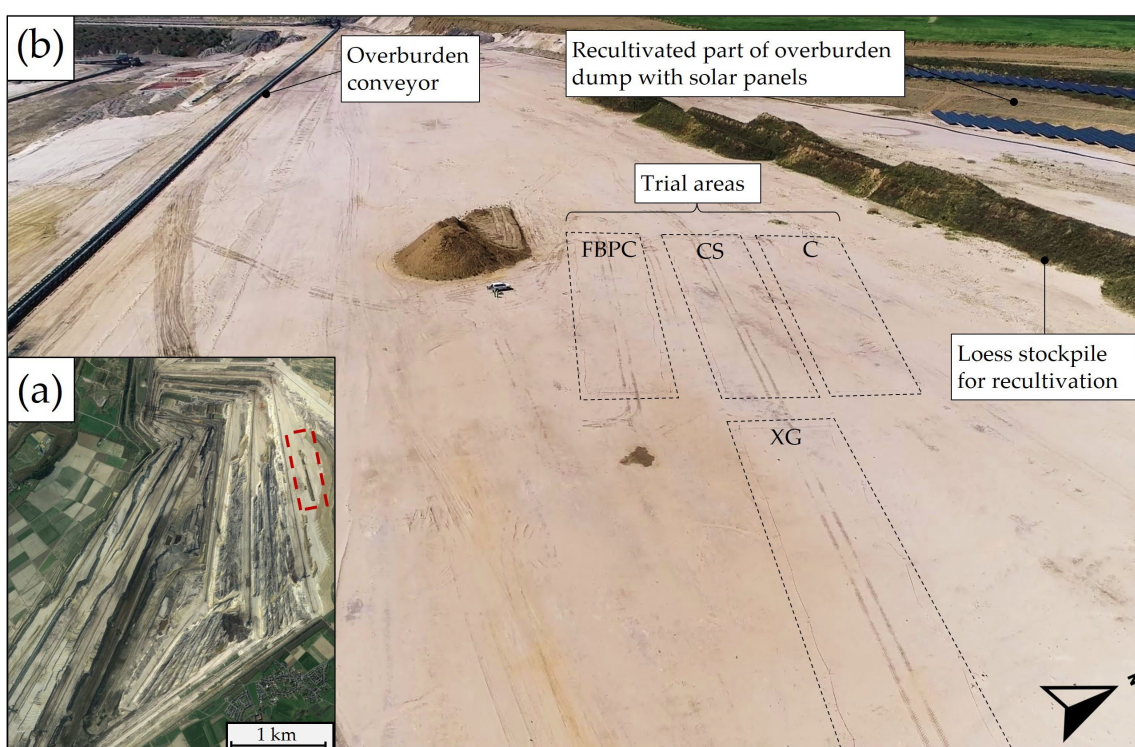


**Figure 1.** (a) Satellite image of the Inden lignite open-cast mine with the field trial location indicated by a red-lined dashed box. Adapted from Google Maps [40]. (b) Drone footage of the field trial location, with prepared trial areas indicated by dashed boxes. Biopolymer-treated areas: FBPC, CS, and XG; untreated control: C.

Substrate properties (i.e., geochemistry, mineralogy, specific gravity, pH, and soil colour, Tables 1 and 2) were established on a single composite sample generated by blending subsamples from all four trial areas. Geochemical composition of the composite sample was determined at ALS Geochemistry (Loughrea, Ireland), which performed whole-rock analysis using X-ray fluorescence spectroscopy (XRF) and inductively coupled plasma mass spectrometry (ICP-MS) with four-acid digestion. Its mineralogy was established by semi-quantitative X-ray diffraction (XRD) using an AERIS benchtop XRD (Malvern Panalytical) instrument with a Co LFF tube (Institute of Mineral Resources Engineering, RWTH Aachen University, Aachen, Germany). Results demonstrate that the composite material consists primarily of quartz and orthoclase.

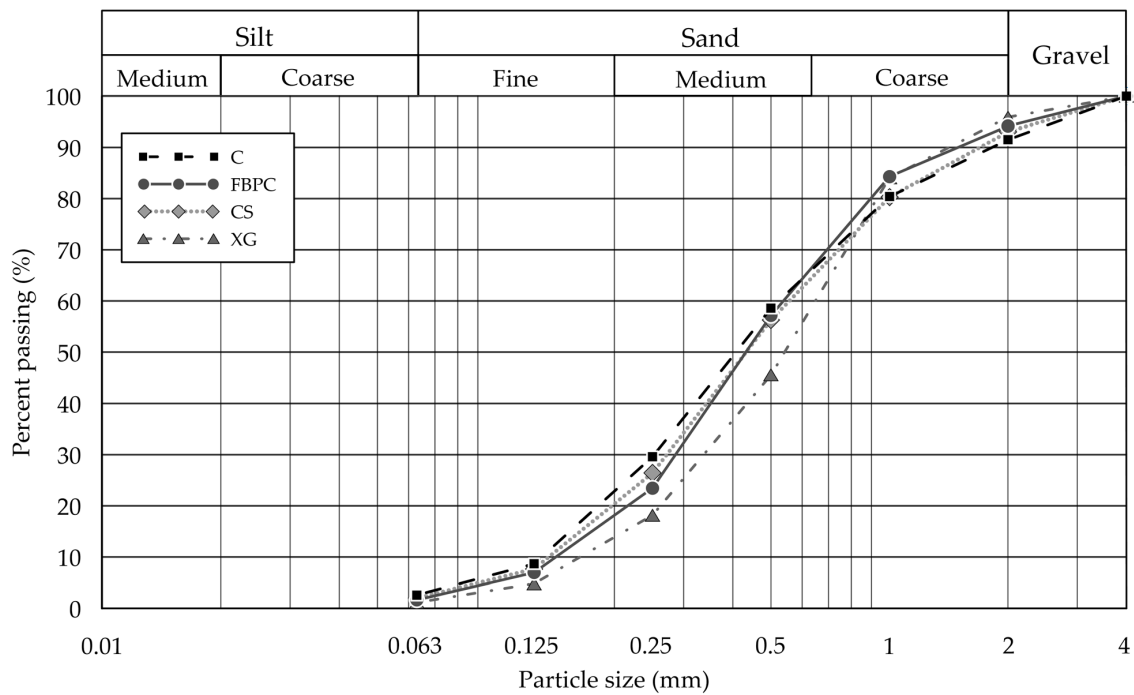


**Figure 2.** Particle size distribution of mine soils from different trial areas. C = control, CS = corn starch, FBPC = fava bean protein concentrate, XG = xanthan gum.

**Table 1.** Soil properties of biopolymer-treated (FBPC, CS, and XG) and untreated control (C) trial areas.

Parameter	Unit	Test Fields						Method
		C	FBPC	CS	XG	M	SD	
D <sub>60</sub>	mm	0.52	0.54	0.56	0.64	0.57	0.05	DIN EN ISO 17892-4 [39]
D <sub>50</sub>	mm	0.41	0.44	0.44	0.55	0.46	0.05	DIN EN ISO 17892-4 [39]
D <sub>30</sub>	mm	0.25	0.29	0.28	0.33	0.29	0.03	DIN EN ISO 17892-4 [39]
D <sub>10</sub>	mm	0.13	0.14	0.13	0.18	0.14	0.02	DIN EN ISO 17892-4 [39]
C <sub>u</sub>	-	4.16	3.86	4.31	3.56	3.97	0.29	DIN EN ISO 17892-4 [39]
C <sub>c</sub>	-	0.96	1.11	1.08	0.95	1.02	0.07	DIN EN ISO 17892-4 [39]
USCS	-	SP				ASTM D-2487 [41]		
Specific gravity	g/cm <sup>3</sup>	2.66				DIN EN ISO 11508:2018-04 [42]		
pH value	-	4.60				DIN EN 15933:2012-11 [43]		
Soil colour	Munsell	1.3Y 6.5/1.7						

C<sub>u</sub> = coefficient of uniformity, C<sub>c</sub> = coefficient of curvature, USCS = Unified Soil Classification System, M = mean, and SD = standard deviation.

**Table 2.** Geochemistry of soil composite of all trial areas.

Oxides	Content (wt%)
SiO <sub>2</sub>	95.44
Al <sub>2</sub> O <sub>3</sub>	2.17
K <sub>2</sub> O	1.16
Fe <sub>2</sub> O <sub>3</sub>	0.18
TiO <sub>2</sub>	0.10
Na <sub>2</sub> O	0.07
SO <sub>3</sub>	0.05
CaO	0.04
BaO	0.03
MgO	0.03
P <sub>2</sub> O <sub>5</sub>	0.02

### 2.3. Biopolymer Preparation and Application

The biopolymer concentrations for the treatments were based on a previous laboratory wind tunnel study conducted by Sieger et al. [38]. In that study, the authors determined the ‘plateau concentrations’ of selected biopolymers. These concentrations represent the point above which further increases have an insignificant impact on the treatments’ effectiveness to reduce dust emissions. For the present study, the following plateau concentrations were selected: XG = 0.1 wt%, CS = 0.25 wt%, and FBPC = 0.75 wt%. For these concentrations, the results of the previous wind tunnel study suggest that all treatments will achieve a similar dust suppression performance [38]. In addition, the calculation of the required biopolymer mass accounted for the biopolymer’s respective moisture content (Section 2.1), and each biopolymer solution was applied to the trial areas at an application rate of 0.5 L/m<sup>2</sup>. This resulted in treatment dosages of 0.7 g/m<sup>2</sup> for XG, 1.3 g/m<sup>2</sup> for CS, and 4.1 g/m<sup>2</sup> for FBPC.

A tractor-mounted field sprayer was used to prepare and apply the biopolymer solutions (Table 3 and Figure 3). The solutions were prepared by filling the tank of the field sprayer with the required volume of fresh water, adding the biopolymers via the external filling sluice, and mixing it with the field sprayer’s built-in agitation system for 10 min until completely dissolved. Biopolymer solution of 750 L was required per test area. Constant pumping and spraying rates (L/min) throughout the spraying process were ensured by accounting for an additional 100 L solution in the tank, resulting in a total of 850 L solution prepared and 750 L applied.

**Table 3.** Field sprayer type and relevant application parameters.

Parameter	Value	Unit
Field sprayer model	Holder IS 1000	-
Tank volume	1000	L
Spraying width	15	m
Driving speed	1.1	km/h
Pump rate	69	L/min
Pump pressure	3.5	bar
Application rate per pass	0.25	L/m <sup>2</sup>
Nozzle size (ISO 10625) [44]	05	-
Nozzle count	18	-

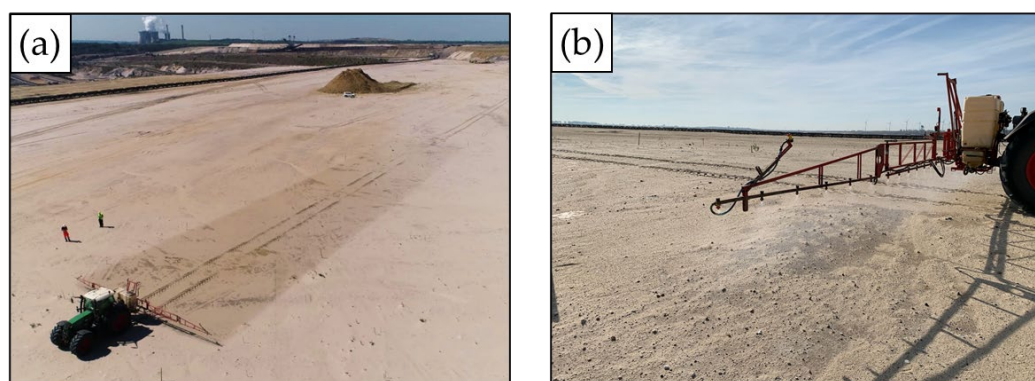


**Figure 3.** (a) Aerial picture of biopolymer application on trial areas. (b) Close-up shot of the field sprayer applying the biopolymer solution.

The biopolymer solutions were applied to the trial areas with the tractor travelling longitudinally across the centre of the test area (Figure 3a). The total required application rate of 0.5 L/m<sup>2</sup> was achieved in two passes (0.25 L/m<sup>2</sup> per pass), with the tractor making a U-turn at the end of the first pass. After initial application on D0, no further re-applications were performed. With a constant pump rate of 69 L/min and a spray width of 15 m, a constant driving speed of 1.1 km/h was required to achieve the 0.25 L/m<sup>2</sup> rate, which was

maintained by the field sprayer's onboard control system. The spraying nozzles produced a fine mist, and no clogging, failure or other malfunction was observed throughout the spraying of any of the biopolymers (Figure 3b). The tank was emptied and rinsed between preparation of the different biopolymer solutions.

#### 2.4. Test Methodology

The field trials started with biopolymer application on day 0 (D0, 8 August 2022) and continued until day 45 (D45, 22 September 2022). During this period, tests were performed on D2, D8, D15, D25, D32, D38, and D45. On each test day, the test programme consisted of:

1. measurements of dust emissions generated by exposing trial plots to a fan-generated airflow (Section 2.5);
2. visual inspection of the trial plots tested in (1.); and
3. penetrometer tests (Section 2.6).

Uniform testing across the trial areas was ensured by dividing the trial areas into separate sections for each test day (Figure 4). The right and left boundaries (each 15 m wide) were not measured and included in the test design in case adjustments to the field sprayer's travel speed and pumping rate were required at the start and end of the spraying process. A weather station located 3 km west of the field trial site provided meteorological data, including precipitation ( $L/m^2$ ), temperature ( $^{\circ}C$ ), relative humidity (%), and maximum wind speed (m/s) for the field trial period.

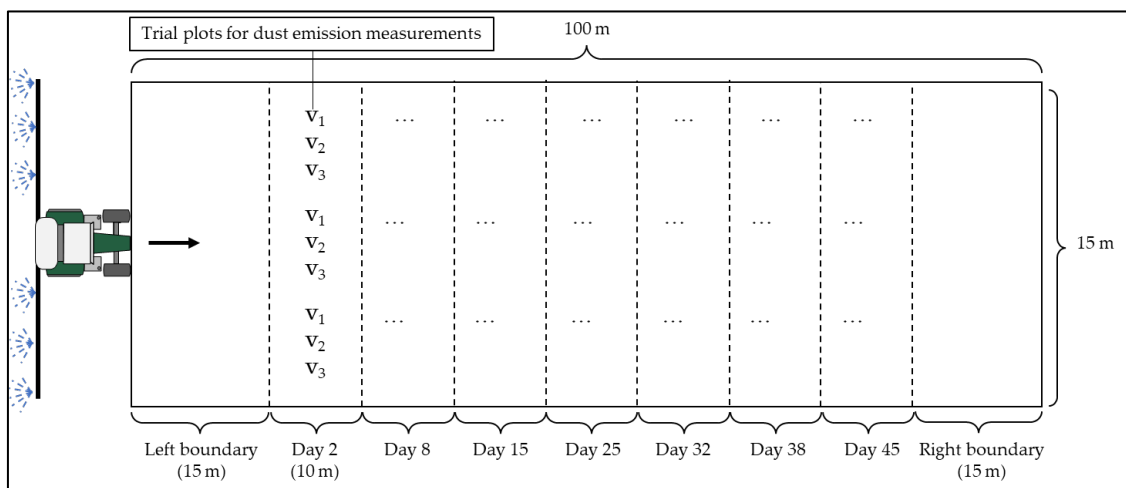


**Figure 4.** Schematic drawing of trial area with its subdivisions for the corresponding test days. Note:  $v_1$ ,  $v_2$ , and  $v_3$  denote indicative locations for the trial plots where dust emission measurements were performed (see Section 2.5).

#### 2.5. Dust Emission Measurements

On each test day, the effectiveness of the different biopolymer treatments was investigated by exposing representative  $70 \times 40 \text{ cm}^2$  plots within the trial areas to different air speeds generated by an electric air blower and measuring the emitted dust emissions with an aerosol spectrometer (Figure 5). Each measurement lasted for 60 s, and a DustTrak 8533 aerosol spectrometer was used to measure particulate matter (PM) emissions of the  $PM_{2.5}$  and  $PM_{10}$  fractions and total suspended particles (TSPs) in  $mg/m^3$ . According to WHO guidelines, PM is a "mixture of solid and liquid particles in the air that are small enough not to settle out on the earth's surface under the influence of gravity, classified by aerodynamic diameter" [45]. The  $PM_{10}$  and  $PM_{2.5}$  fractions represent the mass of soil particles contained in the TSPs, with an aerodynamic diameter  $\leq 10$  and  $2.5 \mu\text{m}$ , respectively.



**Figure 5.** Test setup for dust emission measurements.

The DustTrak 8533 has a lower and upper detection limit of 0.001 and 150 mg/m<sup>3</sup>, respectively, and was set to a sampling rate of 1 Hz and a pump rate of 3 L/min. Prior to the field trials, the instrument was calibrated by the manufacturer to standard ISO 12103-1 [46], A1 test dust. Unbiased sampling was ensured using an isokinetic metal pitot tube with a 90° bend and a 2 mm inlet diameter. The pitot tube was mounted on a tripod 5 cm above the surface and 70 cm away from the electric air blower, facing the opposite direction of the air blow. The wind erosion resistance was investigated by performing tests at three different air velocities, namely,  $v_1 = 13.3$  m/s (48 km/h),  $v_2 = 15.5$  m/s (56 km/h), and  $v_3 = 17.4$  m/s (63 km/h). These velocities represent different preset speed levels of the electric air blower. All tests were performed in triplicate ( $n = 3$ ), and each was conducted on a new trial plot. Background emissions were determined on each test day. After measurements with substantial dust emissions, the aerosol spectrometer was recalibrated and the plastic hose and pitot tube were flushed with pressurised air from the inside. As previously pointed out by Freer et al. [47], such electric air blowers generate turbulent flow and are not directly comparable with portable wind tunnels that simulate the atmospheric flow causing natural wind erosion [48].

A custom-built wooden plate and a U-shaped frame provided reproducible test conditions (Figure 5). The DustTrak and the tripod were mounted to the wooden plate, and the sampling tube was connected to the DustTrak by a plastic hose. The wooden U-frame aligned the pitot tube, trial plot, and fan for each measurement. The U-frame had inner dimensions of 40 × 100 cm<sup>2</sup> and was mounted with a yellow 1 m tapeline. The electric air blower was deliberately positioned at 70 cm to the pitot tube, resulting in a 40 × 70 cm<sup>2</sup> trial plot. In addition, the U-frame provided a reference for taking comparable pre- and post-test photographs. The electric air blower was stabilised and fixed by mounting it to a stainless-steel plate. A top-view picture of each trial plot was taken before and after each wind erosion test to visually compare the effect of the air velocities ( $v_1$ ,  $v_2$ , and  $v_3$ ) and the different trial areas among each other.

### 2.6. Penetrometer Tests

On each test day, a hand-held pocket penetrometer (H-4205) was used to measure the penetration resistance of the surface layers of the trial areas. Tests were performed with a 6.4 mm-diameter flat-ended penetrometer tip. The penetrometer has a load scale from 0 to 108 N and a resolution and lower reading limit of 0.5 N. Tests were performed up to a penetration depth of approximately 1 cm, with 20 replicates at an angle of 90°.

## 3. Results

### 3.1. Meteorological Data

Figure 6 displays the precipitation ( $L/m^2$ ) measured by the local weather station throughout the field trial period, with the day of application and the different test days (T#1–T#7) indicated by black squares. Further meteorological data, including temperature, humidity, and maximum wind velocity, are appended in Table A1. The first small precipitation event of  $0.4 L/m^2$  occurred on the seventh day (D7) after biopolymer application, one day before T#2. Further rainfall of  $4.3 L/m^2$  was recorded between T#2 and T#3. Two days before D25 (T#4), the first large precipitation event,  $6.8 L/m^2$ , took place. The following week, significant rainfall of  $31.4 L/m^2$  occurred from D29 to D31 before T#5 (D32). Ahead of T#6, again, considerable rainfall of  $11.5 L/m^2$  fell between D36 and D38. The subsequent days were also characterised by further rainfall, followed by only slight precipitation of  $0.2 L/m^2$  on D42 and D43 and no rainfall on D44 and D45 (T#7).

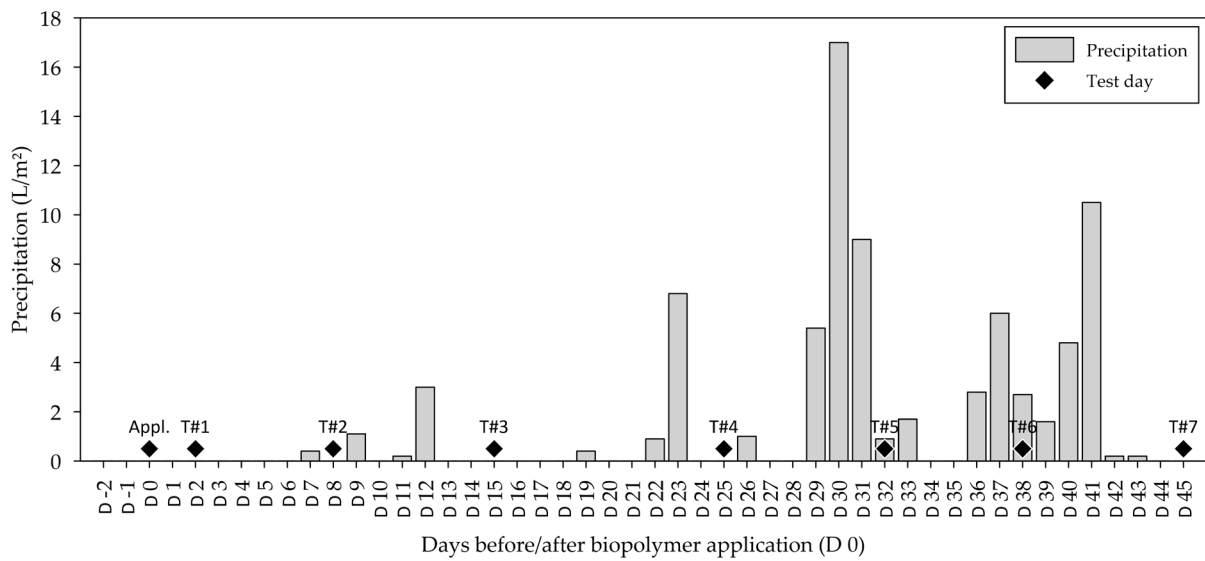


**Figure 6.** Precipitation during the field trials, starting two days before biopolymer application (D –2, 6 August 2022) and lasting until day 45 (D 45, 22 September 2022). Note: the numerical values are appended in Table A1. Appl. = date of applying biopolymers.

### 3.2. Dust Emission Measurements

#### 3.2.1. Time Series of Individual Measurements

Figure 7 shows the time series of the TSP concentrations measured during the dust emission tests performed on D2 at air speeds of  $v_1$ ,  $v_2$ , and  $v_3$ . Irrespective of the velocities tested, the control group (C) showed significant mean TSP emissions (at  $v_1 = 49.1 mg/m^3$ ,  $v_2 = 36.08 mg/m^3$ , and  $v_3 = 28.04 mg/m^3$ ), while all biopolymer-treated plots exhibited considerably lower emissions ranging between 0.05 and  $0.43 mg/m^3$ . The measured emissions typically peaked in the first 3 to 10 s, whereafter they gradually decreased, a trend that generally applied to all tests throughout the field trials. On D2 and a few other test days, emissions from the untreated control reached the DustTrak’s upper detection limit of  $150 mg/m^3$  for several seconds when exposed to air velocities  $v_2$  and  $v_3$ . It is assumed that the actual emissions during these events were above the detection limit. As

shown in Figure 7, emissions tended to reduce more rapidly at higher air velocities (e.g.,  $v_2$  and  $v_3$  on the untreated control).

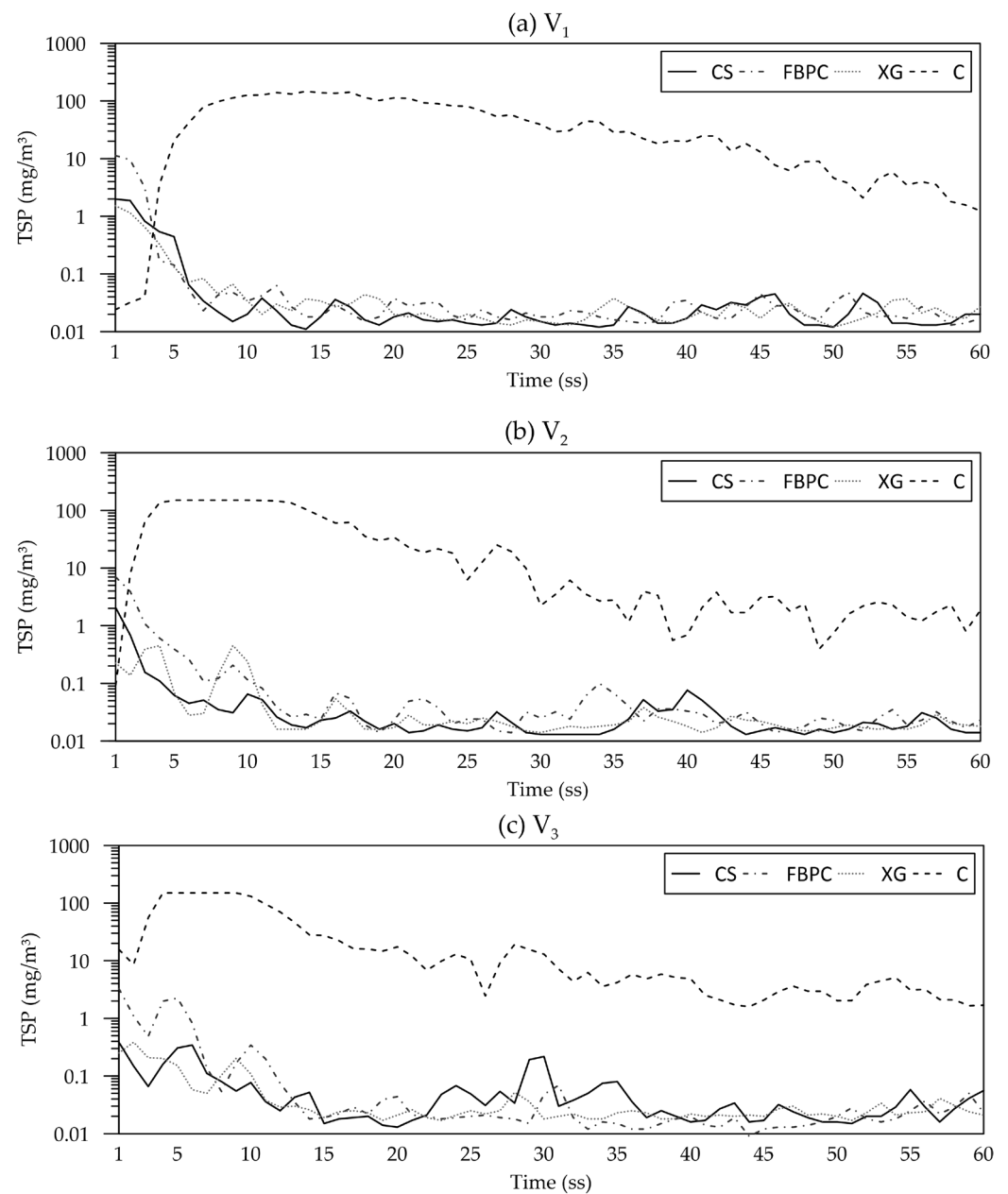


**Figure 7.** Time series of TSP emissions measured on the first test day (T#1) two days after the biopolymer solution was applied (D2). Tested wind velocities: (a)  $v_1 = 13.3$  m/s, (b)  $v_2 = 15.5$  m/s, and (c)  $v_3 = 17.4$  m/s.

### 3.2.2. Temporal Development throughout the Field Trials

Figure 8 shows the results of the (a) TSPs, (b)  $PM_{10}$ , and (c)  $PM_{2.5}$  emissions measured on trial plots exposed to  $v_1 = 13.3$  m/s. The corresponding results for dust emission measurements performed at  $v_2 = 15.5$  m/s and  $v_3 = 17.4$  m/s are displayed in Figures 9 and 10. The dust emissions measured on the untreated and biopolymer-treated trial plots varied significantly throughout the field trials. In contrast, the recorded background load remained consistently low, with TSPs ranging from 0.02 to 0.05  $mg/m^3$ . The results from the trial plots exposed to air speeds of  $v_1$ ,  $v_2$  and  $v_3$  show similar overall trends. The following paragraphs describe the temporal development of the dust emissions measured throughout the field trials for plots exposed to air flows at  $v_1$ .

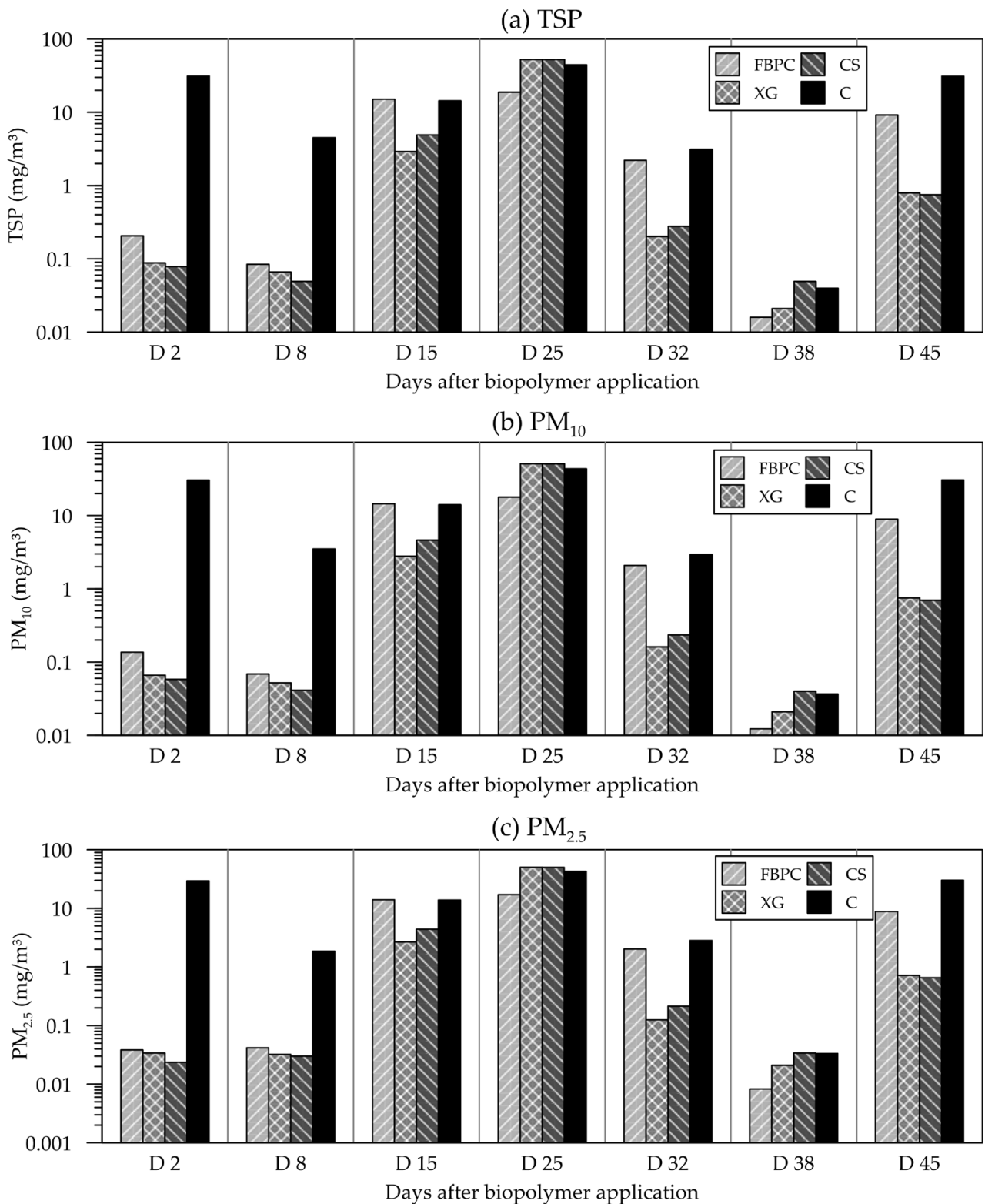


**Figure 8.** Mean dust emissions measured on untreated control (C) and biopolymer-treated trial plots exposed to air speed of  $v_1 = 13.3$  m/s. (a) TSPs, (b) PM<sub>10</sub>, (c) PM<sub>2.5</sub>. Biopolymer treatments were applied at 0.5 L/m<sup>2</sup> and concentrations for FBPC = 0.75 wt%, CS = 0.25 wt%, and XG = 0.13 wt%. Tests were performed in triplicate ( $n = 3$ ), and numerical data of the test results, including mean (M) and standard deviation (SD), are appended in Table A2.

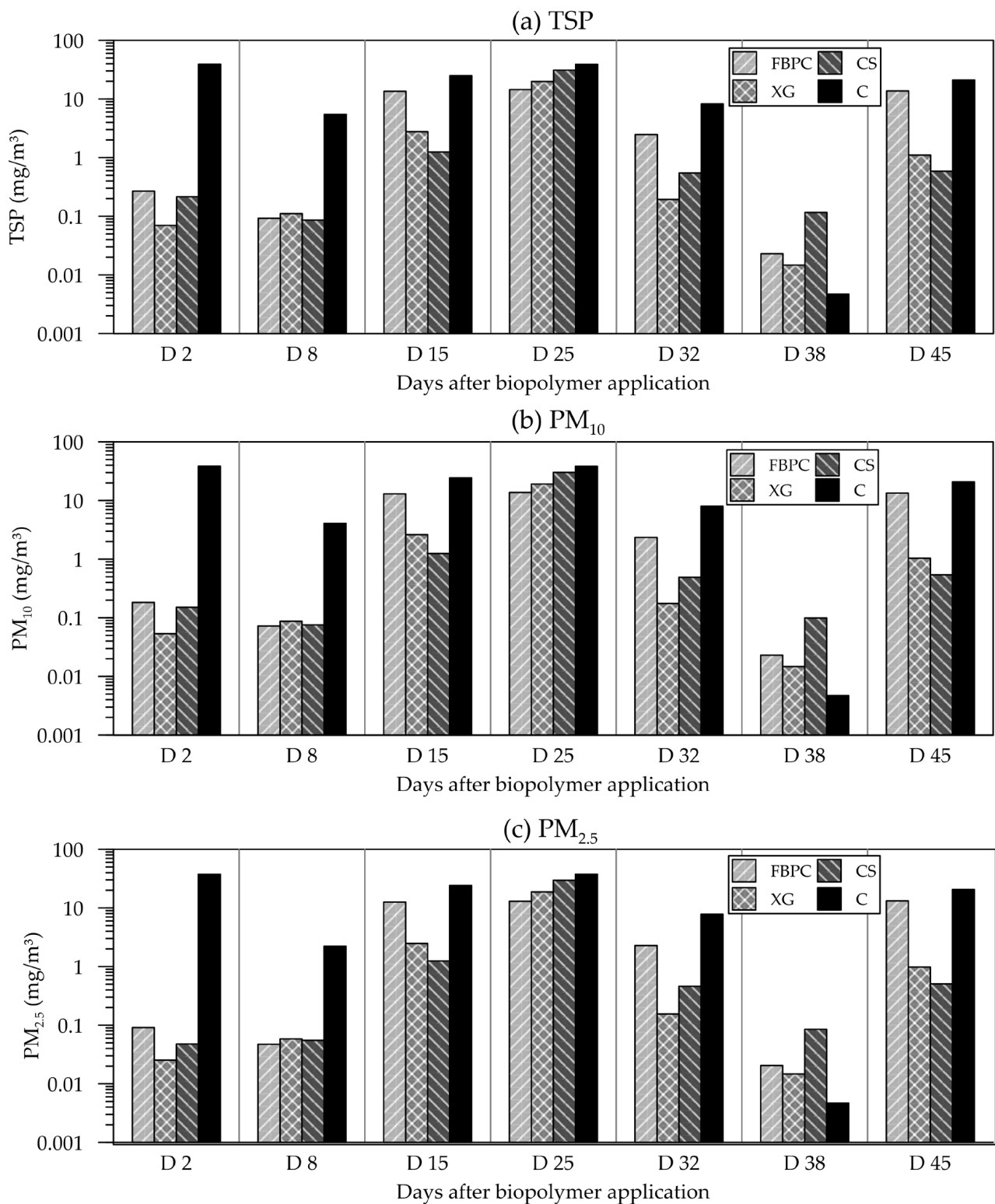


**Figure 9.** Mean dust emissions measured on untreated control (C) and biopolymer-treated trial plots exposed to air speed of  $v_2 = 15.5$  m/s. (a) TSPs, (b) PM<sub>10</sub>, (c) PM<sub>2.5</sub>. Tests were performed in triplicate ( $n = 3$ ), and numerical data of the test results, including mean (M) and standard deviation (SD), are appended in Table A3.

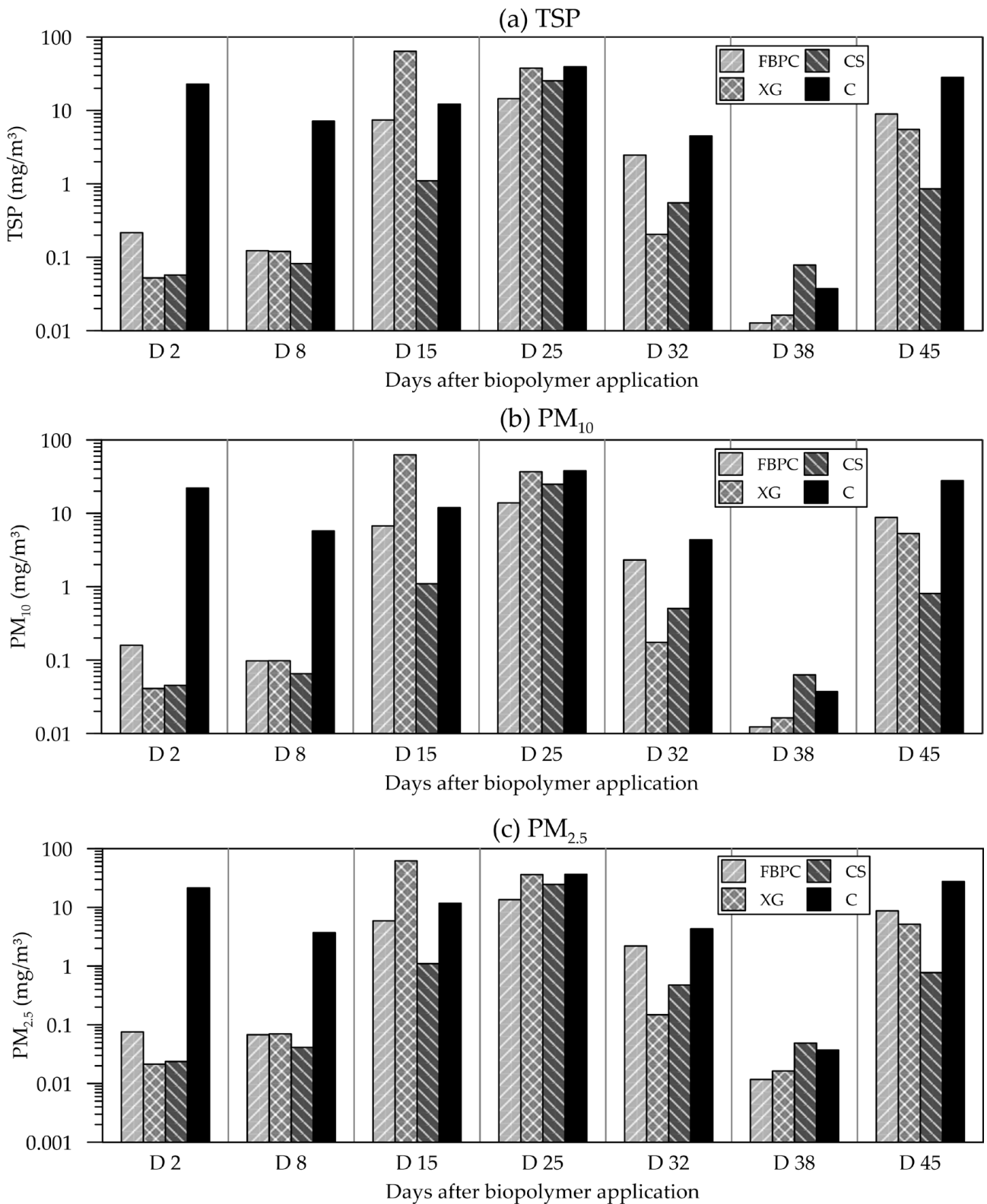


**Figure 10.** Mean dust emissions measured on untreated control (C) and biopolymer-treated trial plots exposed to air speed of  $v_3 = 17.4$  m/s. (a) TSPs, (b) PM<sub>10</sub>, (c) PM<sub>2.5</sub>. Tests were performed in triplicate ( $n = 3$ ), and numerical data of the test results, including mean (M) and standard deviation (SD), are appended in Table A4.

*Temporal Development of Dust Emissions of Trial Plots Exposed to  $v_1$  (see Figure 8):*

- *D2 and D8.* Here, the biopolymer-treated trial plots (CS, FBPC, and XG) exhibited low dust emissions, while significant emissions were measured on the untreated plots. Mean TSP emissions of the biopolymer-treated plots ranged from 0.05 to 0.21 mg/m<sup>3</sup>, while emissions from the control section (C) ranged from 4.5 to 31.2 mg/m<sup>3</sup>. Among the biopolymer treatments, the FBPC-amended test sections exhibited slightly higher emissions than the XG- and CS-amended ones.
- *D15 and D25.* Compared to the first two test days, the results of D15 and D25 showed different behaviour, as dust emissions gradually increased across all trial plots. On D15, the observed TSP emissions from the biopolymer-treated plots increased notably (CS: 4.9 mg/m<sup>3</sup>, FBPC: 15.1 mg/m<sup>3</sup>, and XG: 2.93 mg/m<sup>3</sup>), with the FBPC-amended plots displaying similar emissions to the control (C: 14.3 mg/m<sup>3</sup>). The peak emissions of the study were recorded on D25, whereby the FBPC-treated plots exhibited lower TSP emissions (18.8 mg/m<sup>3</sup>) than the other plots (CS: 52.4 mg/m<sup>3</sup>, XG: 52.5 mg/m<sup>3</sup>, C: 44.5 mg/m<sup>3</sup>).
- *D32 and D38.* On D32 and D38, the measured emissions decreased, reaching the field trial's low point on D38. Compared to D25, all trial plots exhibited relatively low TSP emissions on D32 (CS: 0.3 mg/m<sup>3</sup>, XG: 0.2 mg/m<sup>3</sup>, FBPC: 2.2 mg/m<sup>3</sup>, and C: 0.1 mg/m<sup>3</sup>). On D38, emissions decreased even further, with only marginal TSP emissions measurable on all plots (CS: 0.05 mg/m<sup>3</sup>, FBPC: 0.02 mg/m<sup>3</sup>, XG: 0.02 mg/m<sup>3</sup>, and C: 0.03 mg/m<sup>3</sup>).
- *D45.* On the last test day, the measured emissions had increased considerably compared to D38 (CS: 0.75 mg/m<sup>3</sup>, FBPC: 9.18 mg/m<sup>3</sup>, XG: 0.79 mg/m<sup>3</sup>, and C: 31.0 mg/m<sup>3</sup>). Therefore, the control exhibited the highest emissions.

*Comparison of TSP Emissions between the Trial Plots Exposed to  $v_1$ ,  $v_2$ , and  $v_3$ :*

- *Overall behaviour:* Dust emissions of tests performed at  $v_2$  and  $v_3$  display a similar temporal development to that previously described for  $v_1$ . Again, tests on D2 and D8 showed low emissions on the biopolymer-treated plots and high emissions on the untreated plots, followed by dust emissions increasing on D15 and peaking on D25. After that, emissions decreased on D32, bottomed out on D38, and increased again on D45.
- *Comparison of  $v_1$  with  $v_2$  and  $v_3$ :* On D2 and D8, the average emissions induced by air speed of  $v_2$  mostly increased slightly compared to  $v_1$ , while increasing the velocity to  $v_3$  mostly resulted in a decrease compared to  $v_2$ . By contrast, on D15 and D25, the TSP emissions at  $v_2$  on the biopolymer-treated plots were mostly lower than at  $v_1$ . Notably, on D15, the XG-treated plots subjected to  $v_3$  showed considerably higher emissions than the other tested fields. On D32, emissions decreased on all the plots tested and bottomed out on D38, irrespective of the velocity tested. Lastly, on D45, the CS- and XG-treated plots exposed to  $v_2$  displayed similar emissions as  $v_1$ , whereas emissions measured for FBPC-treated plots were increased.

*Conclusion:* A comparison of the results for the different velocities did not reveal a clear trend regarding the effect of air speed on the measured dust emissions.

### 3.2.3. Share of PM<sub>10</sub> and PM<sub>2.5</sub> Fractions

Throughout the field trials, PM<sub>10</sub> and PM<sub>2.5</sub> emissions followed a similar temporal development to that described for TSPs. PM<sub>10</sub> emissions accounted for 89 % (SD = 9) of the TSP emissions measured on plots exposed to  $v_1$ . In addition, 76% (SD = 24) of the recorded TSP emissions were associated with the PM<sub>2.5</sub> fraction. The percentage allocation of the TSP emissions to the PM<sub>10</sub> and PM<sub>2.5</sub> emissions was similar for the tests carried out at  $v_2$  and  $v_3$ . This implies that most of the measured emissions belong to the PM<sub>2.5</sub> fraction.

### 3.2.4. Conclusions

Irrespective of the velocity tested, all biopolymer-treated trial plots showed significantly reduced dust emissions on D2 and D8, while the untreated plots exhibited significant emissions. On the subsequent test days, all trial plots showed a similar overall development. The control (C) showed the highest emissions on almost all test days and was only matched by the FBPC-treated plots on D15 and D32 and the CS- and XG-amended plots on D25. A direct comparison of the biopolymer amendments revealed that the XG- and CS-treated plots showed similar emission behaviour, mainly exhibiting lower emissions than the FBPC-treated plots (i.e., on D2, D8, D15, D32, and D45). Most of the TSP emissions were attributed to the PM<sub>2.5</sub> fraction. Finally, although the measured dust emissions differed for the velocities tested, no clear trend could be identified regarding the effect of the velocity on the measured dust emissions.

### 3.3. Visual Inspection of Trial Plots

While closer inspection of the biopolymer-treated trial areas revealed that the sand particles agglomerated to a surficial crust, it was impossible to take intact crust samples or perform crust thickness measurements, as the formed crusts were too fragile and brittle. Figures 11 and 12 show representative photographs of the trial plots taken after the dust emission measurements at  $v_1 = 13.3$  m/s. Corresponding photographs of the trial plots subjected to  $v_2$  and  $v_3$  are appended in Figures A1–A4. The following paragraphs describe the visual characteristics that can be discerned from the photographs. In general, most of the visually detectable wind erosion occurred during the first few seconds of each test. Saltation appears to be the dominant erosion mechanism, with particles close to the electric fan being eroded by air and their saltation causing further erosion down the line of airflow. The higher the velocity tested, the faster the erosion process.

- *Untreated trial plots (C)*. The fan-generated air flow caused significant erosion on the untreated trial plots, resulting in distinct cone-shaped wind erosion traces on each testing day. The widths and lengths of the erosion traces slightly varied throughout the test days, with less erosion being perceived on D8 and D38 (for  $v_1$ ). On D32, the erosion traces resulting from tests at  $v_2$  and  $v_3$  were slightly bent due to cross-winds. The dimensions of the erosion traces increased significantly with the higher velocities tested (Figures A1 and A3).
- *FBPC-treated trial plots*. On D2, only a few sand particles were eroded by the induced airflow, regardless of the velocity tested, whereas tests on D8 produced visually perceivable erosion marks. From D15 onwards, the typical cone-shaped erosion traces became visible, becoming larger and more distinct with each measurement day. However, throughout the field trials, the erosion traces on the FBPC-treated soil ( $v_1$ ) were smaller than the corresponding traces on the untreated plots. In contrast, the  $v_2$  and  $v_3$  trials resulted in more similar erosion traces.
- *CS-treated trial plots*. Similarly to the FBPC-treated plots, almost no erosion traces were observed after the tests on D2 and D8, regardless of the velocity tested. On D15, the induced airflow produced clearly visible erosion traces, but not as distinct or large as the corresponding untreated plots (for  $v_1$ ,  $v_2$ , and  $v_3$ ). From D25 onwards, the CS-treated plots exhibited erosion traces of similar shape and size to the untreated plots at all velocities tested.
- *XG-treated trial plots*. Similarly to the CS- and FBPC-treated trial plots, the XG-treated plots showed almost no wind erosion throughout the tests on D2 and D8 at all velocities. However, on D8, the XG-treated plots displayed slightly larger erosion traces than the CS- and FBPC-treated plots. From D15 onwards, the conical erosion traces could be observed at all velocities tested, and their size increased with each test day. However, the traces were not as distinct or large as the corresponding untreated trial plots.

*Conclusion.* Regardless of the velocity tested, all biopolymer-treated trial plots showed only marginal erosion on D2 and D8, whereas the control showed substantial erosion. From D15 onwards, the biopolymer-treated trial plots also began exhibiting cone-shaped erosion traces similar to those of untreated plots. However, until the end of the field trials, these traces were mainly smaller and less distinct. The lengths and widths of the cone-shaped erosion traces increased with higher air velocities tested.

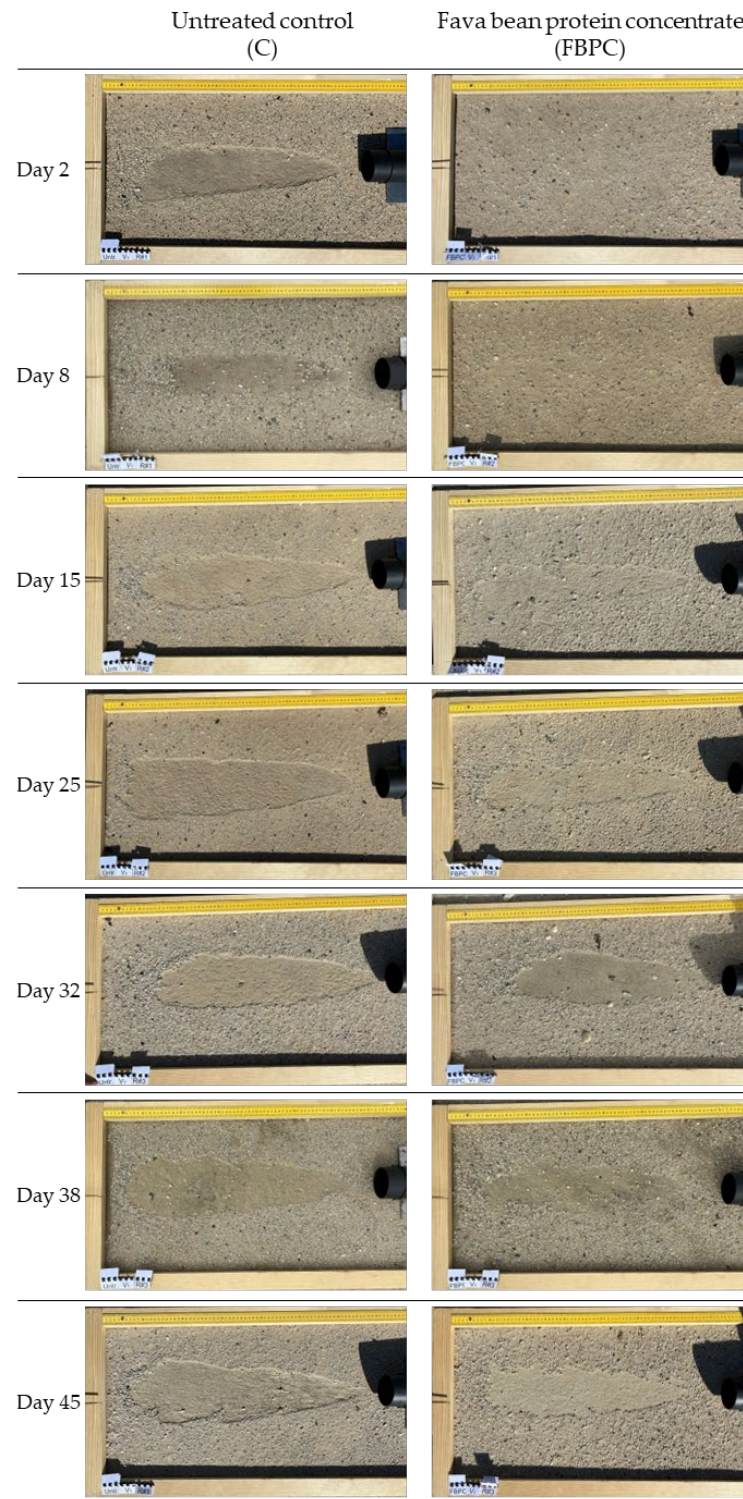


**Figure 11.** Exemplary photographs of plots on the untreated and FBPC-treated trial areas after subjecting them to air speed of  $v_1$  (13.3 m/s) for 60 s. The trial plots had dimensions of  $40 \times 70 \text{ cm}^2$ .

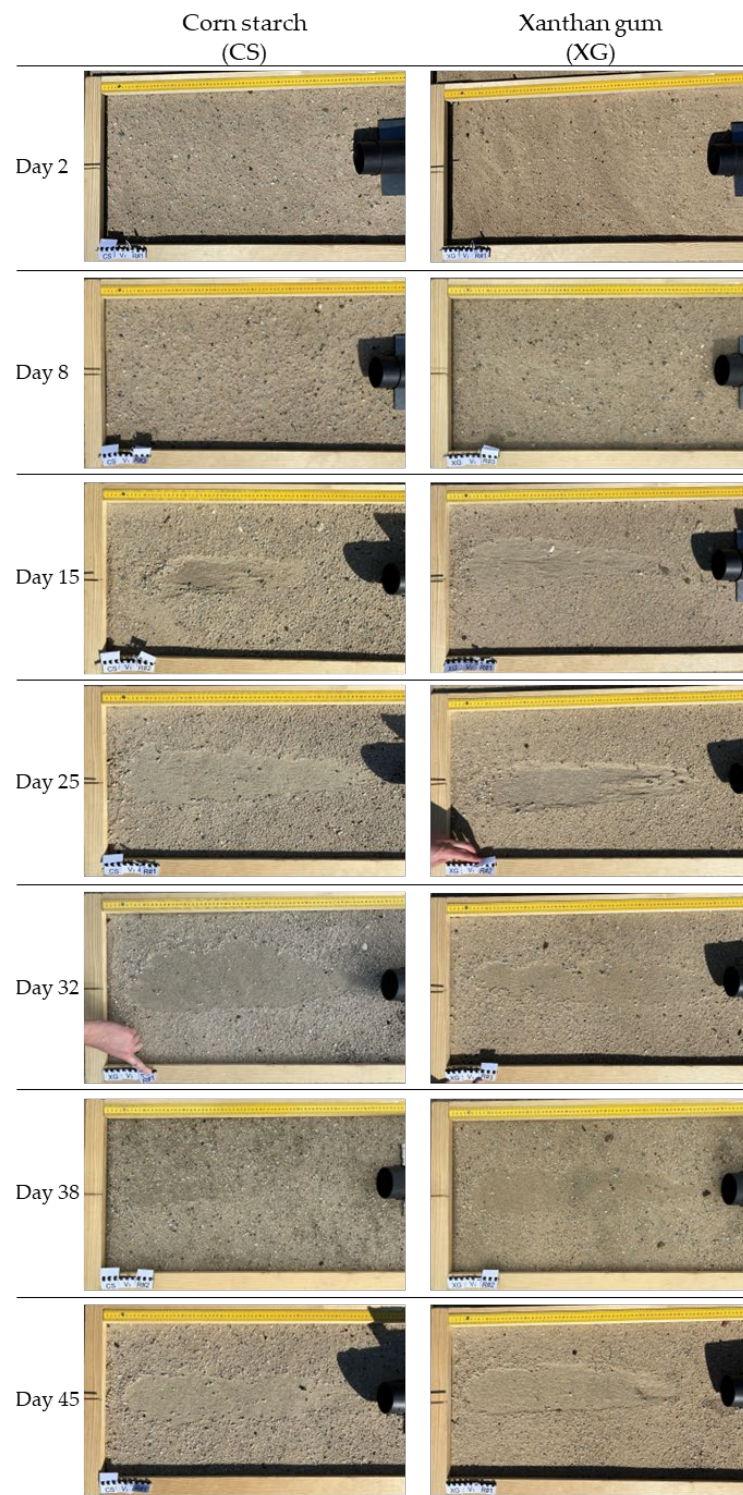


**Figure 12.** Exemplary photographs of CS- and XG-treated trial plots after subjecting them to air speed of  $v_1$  (13.3 m/s) for 60 s. The trial plots had dimensions of  $40 \times 70 \text{ cm}^2$ .

### 3.4. Penetration Resistance

Figure 13 shows the results of the pocket penetrometer tests performed on the trial areas. The top  $\sim 1 \text{ mm}$  of the sand was typically relatively loose on most test days and trial areas, with the penetration resistance increasing below this point. Throughout the field trials, the untreated trial areas exhibited relatively low penetration resistance ranging from 3.2 to 3.6 N on D2, D8, and D15, and increased slightly from D25 onwards. By

contrast, the biopolymer-treated trial areas displayed increased penetration resistance on D2 and D8, ranging from 6.7 to 20.3 N, which decreased significantly from D15 onwards. The CS-treated trial areas displayed the highest penetration resistance until D8. After that, it dropped to a level similar to the untreated area. The FBPC-treated area showed high resistance until D8 (18.8 N) and halved to 9.8 N on D15. However, it still exhibited the highest resistance until D38 (8.2 N), reaching a similar level as the other trial areas (D38: XG = 5.4, CS = 7.3, and C = 6.7 N). The XG-treated trial areas showed elevated resistance that gradually decreased until D15. From there on, it exhibited a similar trend as the untreated area. In general, the penetration resistance on all areas exhibited relatively high variability, as reflected in the standard deviations of the test results (Table A5).

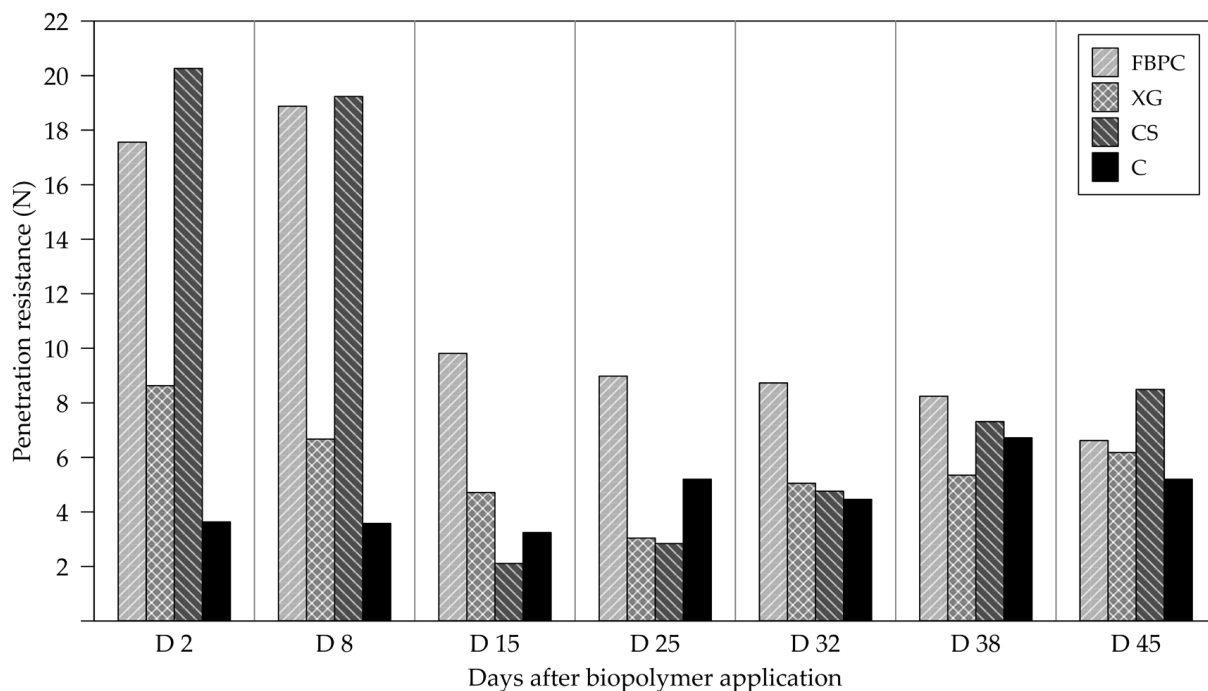


**Figure 13.** Mean penetration resistance of untreated control (C) and biopolymer-treated trial areas. Biopolymer treatments were applied at 0.5 L/m<sup>2</sup> and concentrations for FBPC = 0.75 wt%, CS = 0.25 wt%, and XG = 0.13 wt%. Tests were performed with replicates ( $n = 20$ ), and numerical data of the test results, including mean (M) and standard deviation (SD), are appended in Table A5.

## 4. Discussion

### 4.1. Findings from Previous Field Trials

Several previous field trials have examined the application of dust suppressants. Some have investigated their application on unpaved roads, where traffic-related mechanical disturbance is the primary source of dust emissions (e.g., [11,32,49–53]). Others have tested their application on barren, undisturbed areas where wind erosion is the main source of dust emissions (e.g., [54–57]). As the present field trials investigated the dust emissions from undisturbed, biopolymer-treated areas exposed to airflow, this discussion focuses on the latter. In the following, the main results of previous field trials are summarised, and their key parameters and findings have additionally been compiled in Table A6.

Previous field trials by Park et al. [54], Freer et al. [47], and Shen et al. [57] tested diverse substances and application parameters on different soil types and areas. They found that the treatments allowed effective short-term suppression of dust emissions (Table A6). Park et al. [54] applied poloxamer (amphiphilic copolymer) on tailings storage facility slopes and beaches, reporting significantly reduced PM<sub>10</sub> emissions one week after application, but almost no residual effect in the second week. Freer et al. [47] tested different food-processing by-products and reported considerable short-term emission reductions up to 14 days after application. Shen et al. [57] reported an efficacy of over one month

when testing a starch-polyacrylamide mixture on loess soil. All these studies attributed the degradation of the treatments' effectiveness to rainfall, leaching the substances from the soil surface.

In contrast to these treatments with relatively short-term effectiveness, the highest durability of a treatment was reported by Kavouras et al. [56], who tested tall oil pitch on sandy loam and reported significantly reduced PM<sub>10</sub> emissions over 3 to 6 months. The high durability of the treatment was probably due to the high dosage tested (concentration: 14 to 17% and application rate: 2 L/m<sup>2</sup>) and the fact that tall oil has a higher water resistance than other organic treatments [58]. Contrary to the results reported in these previous studies, only Preston et al. [55] observed no clear effect in their field trials with different dust suppressants on tailings soils and attributed this mainly to the field conditions (especially precipitation).

Further in-depth analysis of the field trials in terms of how the effectiveness and durability of a treatment are affected by parameters, such as the suppressant type, application rate, and concentration, is limited due to differences in the trials' test conditions and methods (e.g., soil properties, weather, and test method). The fact that the field trial results are not simply comparable underlines the value and need for repeated field trials to determine suitable suppressant types and application parameters for a given soil type and location. As a direct comparison of data from the documented field trials and those of other studies is impossible, the following discussion focuses primarily on interpreting the results of the present field trials.

#### 4.2. Interpretation of Field Trial Results

##### 4.2.1. Dust Emissions

The results of the field trials were analysed by cross-referencing the measured airflow-induced dust emissions (Section 3.2) with the precipitation data (Section 3.1), the visual inspection observations (Section 3.3), and the penetrometer test data (Section 3.4), and are presented in the following paragraphs. The interpretation focuses primarily on the main trends observed, as a more detailed comparison of the absolute test results is limited by the naturally inherent heterogeneity (e.g., moisture, particle size, and compaction) of the trial areas, spanning 6000 m<sup>2</sup>.

*D2 and D8.* At the start of the field trials, the biopolymer treatments were applied in dry field conditions (D0), with no rainfall recorded until the first test day (D2) and only marginal rainfall one day before the second test day (D8). During the dust emission measurements on D2 and D8, the biopolymer-treated trial plots (FBPC, XG, and CS) exhibited only marginal dust emissions, regardless of the air velocity tested ( $v_1$ ,  $v_2$ , and  $v_3$ ). In contrast, the untreated plots (C) showed significant emissions. These results are consistent with the visual observations, which showed marginal erosion traces on the biopolymer-treated plots, while untreated plots displayed substantial cone-shaped traces (Figures 11, 12 and A1–A4). Thus, all the biopolymer treatments tested significantly increased the wind erosion resistance of the trial plots, resulting in marginal dust emissions. In addition, the penetrometer test results showed enhanced penetration resistance of the biopolymer-treated trial areas (Figure 13), demonstrating the biopolymer treatments' underlying effect. The biopolymers acted by coating the sand particles with a thin film, forming a linked network between soil particles and the biopolymers [59]. During the curing period, the biopolymer solutions dehydrate, and the interparticle cohesion of the biopolymer–soil matrix increases, improving the wind erosion resistance of the soil [35,59,60].

*D15 and D25.* The first significant rainfall, 4.3 L/m<sup>2</sup>, occurred between the second and third test days (D8 to D15), followed by a further 8.1 L/m<sup>2</sup> between the third and fourth test days (D15 to D25). On the actual test days, the soil conditions in the trial areas were dry, indicating that the precipitation had either evaporated or percolated below the soil surface. The dust emissions measured on the biopolymer-treated plots had increased significantly compared to D8 and reached similar or partially even higher levels than the untreated plots (Figures 8–10). It can be concluded that the significant increase in dust emissions is related

to the degradation of the treatments' effectiveness due to rainfall-induced leaching of the water-soluble biopolymers. The visual inspections also revealed cone-shaped erosion traces on the biopolymer-treated plots, with the footprint of these traces increasing from D15 to D25 (Figures 11 and 12). However, on both days, the extent and depth of the traces were not as pronounced as on the untreated plots (Figures 11, 12 and A1–A4). The penetration resistance measured on the XG-, CS- and FBPC-amended plots also decreased to levels similar to the control, with only the FBPC-amended area still showing elevated resistance.

Although the dust emissions increased significantly on D15 and D25, a closer analysis of the emissions measured for the biopolymer-treated plots indicates that residual effects of the treatments were still present on D15 (for the XG and CS amendments) and probably on D25 (FBPC treatment). On D15, the XG and CS amendments showed lower emissions than the control at all velocities tested, with the XG-treated plot tested at  $v_3$  being the only exception. On D25, the residual effects of the XG and CS treatments appeared to have mostly vanished. By contrast, on D25, the FBPC-amended plots showed notably lower emissions than the control. This is likely due to the moisture retention capacity of FBPC and its higher dosage ( $4.1 \text{ g/m}^2$ ) compared to XG ( $0.7 \text{ g/m}^2$ ) and CS ( $1.3 \text{ g/m}^2$ ). Due to the higher dosage, it had likely not been entirely washed off the surface by rainfall. In addition, Sieger et al. [37] previously found that FBPC displayed increased moisture retention capacity. Thus, it is assumed that the remaining FBPC on the trial area allowed it to retain some moisture from the  $6.8 \text{ L/m}^2$  of rainfall that fell on D23, resulting in slightly reduced dust emissions compared to the control.

*D32.* Between D29 and D31, significant rainfall of  $31.4 \text{ L/m}^2$  occurred, resulting in wet soil on the fifth test day (D32). This increase in soil moisture content resulted in higher penetration resistance across all trial areas (Figure 13). The wet soil conditions also resulted in considerably lower dust emissions measured on D32 (Figures 8–10), as the moisture agglomerated the sand particles. However, natural cross-winds and occasional wind gusts strongly influenced the fan's airflow direction, distorting the results and preventing a more detailed comparison. The Inden mine weather station recorded a relatively high maximum wind velocity of  $10.3 \text{ m/s}$  on D32. The effect of the cross-winds is evident in some of the photographs of plots subjected to  $v_2$  (i.e., XG, CS, and C, Figures A1 and A2) and  $v_3$  (i.e., CS and C, Figures A3 and A4). While the interpretability of the dust emission measurements from D32 is thus limited, the comparison of visual characteristics revealed considerable erosion traces on the biopolymer-treated soil plots, which were still not as pronounced as on the untreated test plot. Hence, the biopolymer treatments probably still had a marginal residual effect on D32.

*D38.* Between test days five and six (D32 to D38), further rainfall of  $11.5 \text{ L/m}^2$  occurred, resulting in even wetter soil conditions, as reflected by the increased penetration resistance compared to D32 (Figure 13). As a result of these wet conditions, only marginal dust emissions were recorded across all trial plots, with mean TSP emissions ranging from  $0.05$  to  $0.12 \text{ mg/m}^3$ , only slightly above the background level ( $0.03 \text{ mg/m}^3$ ). The saturated soil conditions also resulted in only marginal wind erosion traces at  $v_1$ , which became more pronounced at  $v_2$  and  $v_3$ . It is therefore concluded that the very low dust emissions are solely related to the saturated soil, which prevented the generation of dust emissions.

*D45.* Before the last test day,  $17.3 \text{ L/m}^2$  rain fell between D39 and D41, followed by  $0.4 \text{ L/m}^2$  three days before D45. On D45, the surface layer of the trial areas appeared to be relatively dry, while the elevated penetration resistance (Figure 13) indicated that the underlying soil was still moist. The measured dust emissions were relatively high again, whereby the biopolymer-treated plots still showed slightly lower emissions than the control. Visual inspection of the photographs revealed the typical cone-shaped erosion traces, with the biopolymer-treated plots still showing slightly smaller traces than the untreated plots. It is thus concluded that the biopolymer treatments still had a marginal residual effect on the wind erosion resistance, which was insufficient to notably reduce the dust emissions induced by airflow.

*Conclusions.* Interpretation of the field trial results revealed that all biopolymer treatments significantly suppressed the dust emissions for the airflows tested for the short term (up to D8). After D8, rainfall leached the water-soluble biopolymers off the soil surface, degrading the effectiveness of the treatments. The conclusion that rainfall leaching appears to be the main factor impairing the treatments' durability is consistent with previous studies (see Section 4.1 and Table A6). As the dust emission measurements, visual inspections, and penetrometer results still indicated a significant effect of the biopolymer treatments on D8, the effectiveness of the treatments would likely have lasted longer had no rainfall occurred in the following days. From D15 to D45, the biopolymer-treated plots still mostly showed slightly lower dust emissions and smaller erosion traces than the control, indicating a marginal residual effect that was insufficient for effective dust control.

#### 4.2.2. Effect of Air Velocity on Dust Emissions and Soil Erosion

A comparison of the measured dust emissions revealed the same overall behaviour throughout the field trials for all velocities tested. Thus, regardless of the velocity tested, it can be concluded that the biopolymer treatments significantly reduced the dust emissions up to D8 of the field trials. However, a closer analysis of the dust emissions measured for the different velocities did not reveal a clear trend regarding the effect of wind velocity on the measured dust emissions. This does not align with the expected outcome of dust emissions increasing at higher velocities. For instance, on D2 and D8, emissions increased as the velocity increased from  $v_1$  to  $v_2$ , but mostly decreased again at  $v_3$ . On D15 and D25, induced air flows at  $v_2$  and  $v_3$  on the treated plots even tended to result in lower emissions than at  $v_1$ . In contrast, the untreated plots showed higher emissions as the velocity increased from  $v_1$  to  $v_2$  and either decreased (D15) or stagnated (D25) as the velocity was further increased to  $v_3$ .

A possible explanation for the unexpected results described in the previous paragraph was derived from a close analysis of the time series of the individual dust emission test results (Section 3.2.1) and the visual observations (Section 3.3). Figure 7 shows that the measured dust emissions tend to decrease more rapidly with increasing velocity after peaking in the first few seconds of each test. This is likely because most soil erosion, and therefore dust generation, occurs in the first few seconds of each test, eroding most of the wind-susceptible sand particles. Therefore, on the one hand, higher velocities resulted in the wind erosion to increase, as evident by the scale of the erosion traces (Section 3.3), indicating a greater dust generation potential. On the other hand, increasing the velocity also accelerated the wind erosion process and the dissipation of the generated dust, resulting in a rapid decrease in the measured dust emissions. It is assumed that these two counteracting effects, in some cases, resulted in the mean measured dust emissions only changing marginally or even decreasing upon increasing the velocity, despite the increased dust generation. Here, a more enclosed test setup would have prevented the rapid dissipation of the dust generated.

#### 4.2.3. Variability in Dust Emission Data

The results of the field trials partially exhibited a high variability between the replicate measurements (Tables A2–A4). Comparison with previous studies showed this to be common for field trials measuring dust emissions (e.g., [55,56,61,62]). Furthermore, on D15, D25, and D38, where the effectiveness of the biopolymer treatments was already degraded, the emissions measured on the biopolymer-treated plots partially exceeded those of the untreated plots (Figures 8–10). Although this contradicts the expectations, results from field trials by Park et al. [54] and Preston et al. [55] show similar trends. Thus, these unexpected trends appear to be common for field trials measuring dust emissions in field settings, and are likely related to the naturally inherent heterogeneity of each soil plot.

#### 4.3. Penetration Resistance

Several laboratory studies have used penetrometer tests to investigate the penetration resistance of biopolymer-treated soils [19–21,24,25,27,30,38,63], and some have additionally found that the penetration resistance correlates with the wind erosion resistance of the soil [19,21,24,38]. Thus, in the context of laboratory studies, penetrometer tests provide a valuable qualitative indicator for evaluating the potential of a substance to enhance soil wind erosion resistance. However, to date, few field trials have employed penetrometer testing, primarily examining the strength of (biological) soil crusts (e.g., [64–68]). Hence, the value of using the penetrometer in field trials investigating dust suppressants or soil stabilisers has not yet been explored.

Penetrometer analyses in this study revealed that the biopolymer-treated trial areas on D2 and D8 showed notably increased penetration resistance (Figure 13), which correlated with low dust emissions measured on the corresponding plots (Figures 8–10). Vice versa, as dust emissions on the treated plots on D15 and D25 increased due to rainfall-induced degradation of the treatments, the penetration resistance decreased significantly. This indicates that the measured dust emissions tend to be negatively correlated with the penetration resistance, similar to previous laboratory studies that reported a correlation between wind erosion and penetration resistance (i.e., [19,21,24,38]). However, analysis of the subsequent test days showed that this relationship must be examined in the context of the soil conditions. On D32 and D38, the soil surface was wet, resulting in significantly reduced dust emissions and increased penetration resistance, although the effectiveness of the biopolymer treatments had already diminished.

A closer comparison of the penetration resistance showed that it only serves as a relative qualitative indicator of the effectiveness of the treatment, as the differences in penetration resistance between the biopolymer-treated areas are not directly reflected in the dust emissions. For example, on D15 and D25, the FBPC-amended area still showed increased penetration resistance compared to the other areas, while all trial plots displayed similarly high dust emissions. Likewise, on D2 and D8, the XG-treated area had significantly lower penetration resistance than the FBPC- and CS-treated areas, while the respective dust emissions were similarly low on all treated plots. Penetrometer readings are, therefore, rather a supporting indicator for estimating whether a treatment still affects the stability of a treated soil. However, in the context of these field trials, it does not allow inferring differences in the soil erosion resistance between different areas. Thus, it cannot replace the need to conduct airflow-induced dust emission measurements to assess the effectiveness of a treatment.

In this study, the penetrometer analyses provided only limited additional value for interpreting the results of the field trials because they only tested relatively low treatment dosages and a spray-on application, resulting in relatively low resistance and rapid degradation. The method is likely more suitable for field trials testing higher dosages or a mix-in application, where higher resistance can be expected. Regardless, the use of penetrometers is a rapid, low-cost method that provides valuable information on surface soil strength.

#### 4.4. Suitability of Test Method

Previous field trials used different experimental setups to measure airflow-induced dust emissions from naturally crusted or amended soils. Some studies employed portable boundary-layer wind tunnels, which facilitate test conditions that reflect natural wind flow and also shield the trial plot from cross-winds (e.g., [32,48,69]). While they constitute a sophisticated field trial test setup, they are costly, inflexible, and must be custom-built. The patented portable in situ wind erosion lab (PI-SWERL) constitutes an alternative apparatus that has been used successfully in several previous field trials (e.g., [55,56,61,62,70]).

Unlike the portable wind tunnels or the PI-SWERL, the experimental setup used for these field trials was similar to the setups previously used by Park et al. [54] and Freer et al. [47] and followed a rather simplistic approach, as tests were performed in open, unenclosed conditions (Figure 5). However, while this setup allowed visual observation of the wind

erosion process, it also resulted in a more rapid dissipation of dust emissions, limiting the ability to investigate the effect of air velocity on the dust emissions (Section 4.2.2). In addition, the lack of shielding likely distorted measurements performed during heavy cross-winds (Section 4.2.1), so the setup could probably be improved by equipping it with an enclosure. Nevertheless, the experience gained during the field trials and the analysis of the results showed that this setup constitutes a simple, mobile, and flexible method for measuring the wind erosion resistance and dust emissions of amended soils.

#### 4.5. Comparison of Field Trials with Previous Laboratory Studies

These field trials build on previous laboratory studies by Sieger et al., who first assessed the particle agglomeration potential of 14 selected biopolymers by moisture retention, penetrometer, and crust thickness tests [37]. A subsequent wind tunnel study analysed the ability of five previously tested biopolymers to enhance the soil wind erosion resistance [38]. The studies showed that all biopolymers agglomerated the sand particles and enhanced the penetration and wind erosion resistance of the samples, with most of the polysaccharides tested (e.g., XG and CS) proving more effective at lower concentrations than proteins (e.g., FBPC) [37,38].

The present study completes this series of studies by conducting field trials with three of the previously tested biopolymers. Thus, it is important to examine how the results of the laboratory studies compare with those of the field trials. It must be noted that the comparability between the laboratory studies and the field trials is limited because the field trials were conducted in an uncontrolled environment, and unlike the laboratory studies, tested only one dosage for each of the different biopolymers (0.7 g/m<sup>2</sup> for XG, 1.3 g/m<sup>2</sup> for CS, and 4.1 g/m<sup>2</sup> for FBPC). This limits the comparison of the effect of biopolymer type and dosage on the effectiveness of a treatment.

Regardless, it can be concluded that the field trial results confirm the laboratory studies' findings. Up to D8, all biopolymer treatments significantly reduced the dust emissions and showed increased penetration resistance compared to the untreated area. On most test days, the polysaccharide-treated plots (XG and CS) displayed comparable or even lower emissions than the FBPC-treated plots, which were applied at a much higher dosage, indicating that the polysaccharides are more effective at lower concentrations than the protein. The XG tested also tended to be more potent than the CS tested, as it displayed similarly low emissions up to D8, despite being applied at a lower dosage. This shows that the findings of the laboratory studies are coherent with the results of the field trials. However, this conclusion does not render the field trials obsolete. Instead, the significant effect of rainfall (and other field conditions) on the degradation of a treatment's effectiveness underlines the need for field trials to determine suitable biopolymer types and application parameters.

#### 4.6. Application Potential of Tested Biopolymers as Dust Suppressants on Mine Sites

Airflow-induced dust emission measurements are an established method for evaluating the effectiveness of a dust suppressant treatment (e.g., [47,54–57]). The dust emissions tests and visual inspections of these field trials showed that all biopolymer treatments effectively suppressed dust emissions in the short term on undisturbed, barren mine soil. Results on D8 indicated that the treatments would have lasted longer under dry conditions. Further aspects, such as durability, cost-effectiveness, availability, ease of use, and environmental friendliness, must be considered to evaluate the potential of biopolymers as novel dust suppressants. While a comprehensive analysis is beyond the scope of this work, these factors are briefly addressed below.

- *Durability.* Rainfall-induced leaching appears to be the main factor impairing the durability of a treatment. Aside from rainfall, biopolymers' environmental degradability also limits the durability of their applications. By contrast, traditional dust suppressants such as chloride salts [58] or synthetic polymer emulsions (e.g., [50,58]) have shown notably higher durability. This implies that biopolymers require more

frequent rejuvenation intervals than conventional dust suppressants to maintain their effectiveness. However, it should be noted that the dosages tested in this study were relatively low compared to previous field trials (Table A6), and it is assumed that higher dosages would enhance the durability of a treatment.

- *Cost-effectiveness.* A cost-effectiveness analysis must account for costs for the biopolymer, water, equipment, fuel, personnel, and rejuvenation intervals required to maintain the effectiveness of the treatments. This study tested relatively low application dosages (see Section 2.3). Considering indicative bulk prices for the respective biopolymers (XG = 2.0–3.0 USD/kg [71], CS < 1.0 USD/kg [22], and FBPC = 1.4–2.5 USD/kg [72]), the estimated biopolymer costs for the doses tested in this study are XG = 14–21 USD/ha, CS < 13 USD/ha, and FBPC = 57–103 USD/ha. These indicative biopolymer costs per hectare suggest that equipment, fuel, and labour costs and their durability primarily affect the cost-effectiveness of a biopolymer treatment. The test results and product costs also suggest that the polysaccharides tested (CS and XG) are more cost-effective than the protein FBPC. Further field trials are required to determine the long-term application costs of biopolymers. It is important to note that the optimal dosage, durability, and thus application costs are highly dependent on site-specific characteristics, such as climate, precipitation, and the forces acting on the treated areas.
- *Availability, ease of use, and scalability.* The biopolymers tested in this study are readily available in most regions of the world, as they are derived from widely abundant crops such as corn (CS) and fava beans (FBPC) or are commonly used in the oil and gas and food and beverage industries (XG) [22,23,72]. Experience from these field trials has shown that biopolymer solutions can be easily prepared and applied on a large scale using readily available spraying equipment.
- *Environmental friendliness.* The safety data sheets (SDSs) of the corn starch (CS) and fava bean protein concentrate (FBPC) tested classify the substances as food ingredients that do not require classification under European Union Regulation (EC) 1907/2006 (REACH regulation). Similarly, the SDS for technical grade xanthan gum (XG) classifies it as readily biodegradable and not dangerous, so it does not require specific labelling under Regulation (EC) 1272/2008 (CLP Regulation). Based on this information, the biopolymers tested in this study are assumed to be environmentally benign. Conversely, traditional dust suppressants, such as salt brines or petroleum-based products, are not as degradable and may have adverse effects on the surrounding flora and fauna [16,58]. Steevens et al. [73] highlighted that overexposure to some synthetic polymers during the handling and application may be carcinogenic to workers. McTigue et al. [16] concluded that there is a lack of comprehensive, independent environmental and toxicity data for many commercial dust suppressants, whose ingredients often remain proprietary. Finally, synthetic polymer ingredients are still predominantly derived from fossil fuels and—unlike the biopolymers tested—are not bio-based.

Thus, it is concluded that the biopolymers tested have the potential to be applied as dust suppressants for short-term dust control on undisturbed and exposed mine soils. While their effective application will likely require more frequent rejuvenation intervals than commercially available products, they are bio-based, can be considered environmentally friendly, have no proprietary formulations, and are readily available.

## 5. Conclusions

This study evaluated the potential of the biopolymers corn starch (CS), fava bean concentrate (FBPC), and xanthan gum (XG) as dust suppressants on large, undisturbed, exposed mine soils by conducting field trials on an overburden dump of the Inden open-cast lignite mine, Germany. The field trials included measurements of dust emissions generated by exposing trial plots to air blowing from an electric fan, visual inspection of tested plots, and penetrometer tests. Based on the results, the following conclusions are drawn.

1. The results of this study demonstrate that the spray-on application of low biopolymer dosages with a tractor-mounted field sprayer allows the effective application of dust suppressants on a large scale.
2. For dust emission measurements, trial plots were exposed to air velocities of up to 17.4 m/s, and the biopolymer treatments tested effectively suppressed the measured dust emissions in the short term up to 8 days (D8) after application. On D2 and D8, mean total suspended particle (TSP) emissions measured on treated plots ranged from 0.05 to 0.27 mg/m<sup>3</sup>, while emissions on untreated plots ranged from 4.5 to 39.2 mg/m<sup>3</sup>. The findings of the visual inspections and the penetrometer tests support the results of the dust emission measurements. After D8, the effectiveness of the treatments degraded rapidly due to rainfall-induced leaching of the water-soluble biopolymers from the soil surface.
3. The custom-built test setup used to measure the dust emissions from biopolymer-treated soil plots by exposing them to airflow generated by an electric air blower proved to be a simple and flexible method for investigating the wind erosion resistance and dust emissions from soils exposed to variable air speeds.

The results of the field trials provide practical evidence that the spray-on application of biopolymers can effectively mitigate dust emissions on large, exposed, undisturbed mine soils in the short term. The biopolymers tested therefore constitute a promising bio-based and environmentally benign alternative to established traditional dust suppressants.

**Author Contributions:** Conceptualisation, J.L.S. and J.F.; methodology, J.L.S. and J.F.; formal analysis, J.L.S.; investigation, J.L.S.; data curation, J.L.S.; writing—original draft preparation, J.L.S.; writing—review and editing, J.L.S., B.G.L. and J.F.; visualisation, J.L.S.; project administration, J.L.S. All authors have read and agreed to the published version of the manuscript.

**Funding:** This research received no external funding.

**Data Availability Statement:** Data supporting the findings of this study will be made available from the corresponding author upon reasonable request.

**Acknowledgments:** We would like to express our gratitude to RWE Power AG, particularly Dennis-Marc Schier, Eva Thelen, and Klaus Gödde for their invaluable support and enabling us to conduct the field trials at the Inden open-cast lignite mine. Furthermore, we thank the Regional Government Arnsberg, Department 6: Mining and Energy in North-Rhine Westphalia for granting permission to conduct the field trials. We also would like to thank Devrim Gürsel and Philipp Schulte for assisting in characterising the soil samples. Last, the authors would like to thank the anonymous reviewers for their helpful comments and suggestions, which improved the manuscript.

**Conflicts of Interest:** The authors declare no conflict of interest.

## Appendix A

**Table A1.** Meteorological data measured by the weather station of the Inden open-cast lignite mine during the field trials (2 August 2022–21 September 2022).

Day before/after Application	Date	Precipitation (L/m <sup>2</sup> )		Temperature (°C)		Humidity (%)	Wind (m/s)
		Total	Mean	Min	Max	Mean	Max
−6	02 August 2022	0.0	22.6	18.5	25.6	60.4	8.7
−5	03 August 2022	0.0	21.3	15.6	29.0	51.2	9.1
−4	04 August 2022	0.4	29.4	19.1	33.3	41.9	7.1
−3	05 August 2022	3.9	26.9	20.4	32.7	49.9	10.7
−2	06 August 2022	0.0	18.4	14.6	21.9	61.8	10.9
−1	07 August 2022	0.0	18.2	10.4	22.2	50.1	5.8
0—BP Application	08 August 2022	0.0	21.4	10.6	25.4	41.3	6.0
1	09 August 2022	0.0	21.2	11.8	26.0	48.3	7.2
2—Test Day 1	10 August 2022	0.0	22.3	15.1	28.9	46.2	6.6
3	11 August 2022	0.0	25.5	16.9	31.2	38.4	6.5
4	12 August 2022	0.0	27.6	17.6	31.6	32.7	7.1
5	13 August 2022	0.0	25.3	17.4	31.4	32.6	9.5
6	14 August 2022	0.0	27.1	18.3	31.7	33.6	7.6
7	15 August 2022	0.4	27.7	17.8	32.6	36.8	7.4
8—Test Day 2	16 August 2022	0.0	22.1	20.0	25.7	60.7	8.1
9	17 August 2022	1.1	27.4	19.0	31.0	47.9	6.6
10	18 August 2022	0.0	21.7	18.2	24.7	68.0	6.3
11	19 August 2022	0.2	21.5	15.6	26.0	62.0	4.7
12	20 August 2022	3.0	22.0	16.7	25.3	62.6	7.8
13	21 August 2022	0.0	21.6	16.7	24.6	55.7	7.8
14	22 August 2022	0.0	20.6	13.7	24.6	52.5	7.2
15—Test Day 3	23 August 2022	0.0	23.6	15.5	28.1	49.8	4.3
16	24 August 2022	0.0	26.5	16.9	29.9	47.5	6.7
17	25 August 2022	0.0	28.6	18.0	32.9	41.1	4.4
18	26 August 2022	0.0	28.6	18.4	32.8	37.1	5.6
19	27 August 2022	0.4	19.6	18.4	23.6	75.0	6.9
20	28 August 2022	0.0	16.9	14.8	19.3	75.5	4.1
21	29 August 2022	0.0	19.6	15.0	23.6	51.7	7.0
22	30 August 2022	0.9	19.6	11.8	23.4	51.9	5.9
23	31 August 2022	6.8	22.4	16.0	27.8	47.5	7.7
24	01 September 2022	0.0	18.5	15.0	23.8	61.6	6.6
25—Test Day 4	02 September 2022	0.0	21.5	13.6	25.5	48.7	5.8
26	03 September 2022	1.0	20.3	16.2	25.7	42.1	8.4
27	04 September 2022	0.0	21.6	14.5	25.6	54.4	5.9
28	05 September 2022	0.0	23.6	16.1	28.1	48.9	5.1
29	06 September 2022	5.4	25.2	16.4	30.5	38.6	4.6
30	07 September 2022	17.0	24.8	16.0	30.0	44.7	14.5
31	08 September 2022	9.0	20.3	15.5	25.1	58.7	11.7
32—Test Day 5	09 September 2022	0.9	18.3	15.1	21.1	65.1	10.3
33	10 September 2022	1.7	17.2	14.8	19.8	68.5	11.8
34	11 September 2022	0.0	16.8	14.9	19.0	77.3	11.4
35	12 September 2022	0.0	19.9	14.7	22.2	65.1	5.1
36	13 September 2022	2.8	21.3	12.5	27.1	52.1	4.3
37	14 September 2022	6.0	21.9	17.3	25.7	57.4	5.1
38—Test Day 6	15 September 2022	2.7	15.1	13.2	18.1	79.9	4.9
39	16 September 2022	1.6	15.2	12.5	17.6	70.3	5.6
40	17 September 2022	4.8	12.4	9.3	14.6	74.7	10.8
41	18 September 2022	10.5	12.4	9.3	14.7	69.9	9.9
42	19 September 2022	0.2	10.0	8.4	12.5	79.3	12.8
43	20 September 2022	0.2	14.2	8.9	16.7	67.5	8.3
44	21 September 2022	0.0	13.5	9.7	15.5	68.4	6.4
45—Test Day 7	22 September 2022	0.0	14.2	6.8	17.7	59.6	4.6

**Table A2.** Results of dust emission measurements performed at velocity  $v_1 = 13.3$  m/s, including the results of the background load tests.

Day	Biopolymer						ControlC		Background Load	
	CS		FBPC		XG		M	SD	M	SD
	M	SD	M	SD	M	SD				
TSPs (mg/m <sup>3</sup> )										
2	0.08	0.03	0.21	0.17	0.09	0.03	31.23	12.71	0.03	0.00
8	0.05	0.00	0.08	0.02	0.07	0.01	4.50	1.35	0.03	0.01
15	4.91	6.36	15.12	4.82	2.93	3.18	14.34	7.32	0.02	0.01
25	52.43	30.07	18.80	2.11	52.47	22.46	44.47	10.73	0.04	0.03
32	0.28	0.20	2.22	0.20	0.20	0.13	3.12	0.80	0.02	0.00
38	0.05	0.02	0.02	0.01	0.02	0.01	0.04	0.03	0.03	0.01
45	0.75	0.22	9.18	2.94	0.79	0.53	31.03	4.11	0.05	0.00
PM <sub>10</sub> (mg/m <sup>3</sup> )										
2	0.06	0.01	0.14	0.09	0.07	0.03	30.33	12.29	0.02	0.00
8	0.04	0.00	0.07	0.02	0.05	0.00	3.49	1.15	0.03	0.01
15	4.61	5.93	14.50	4.78	2.79	3.04	14.04	7.12	0.02	0.01
25	50.80	29.19	17.87	2.30	50.93	22.22	43.47	10.38	0.04	0.02
32	0.24	0.18	2.08	0.20	0.16	0.12	2.93	0.71	0.02	0.00
38	0.04	0.01	0.01	0.01	0.02	0.01	0.04	0.02	0.03	0.00
45	0.70	0.20	8.94	2.86	0.75	0.50	30.50	4.08	0.04	0.00
PM <sub>2.5</sub> (mg/m <sup>3</sup> )										
2	0.02	0.00	0.04	0.02	0.03	0.02	29.37	11.91	0.02	0.00
8	0.03	0.00	0.04	0.01	0.03	0.00	1.85	0.69	0.02	0.00
15	4.41	5.65	14.01	4.80	2.67	2.97	13.81	6.95	0.01	0.00
25	49.90	28.69	17.13	2.46	49.97	22.06	42.73	10.18	0.02	0.01
32	0.21	0.16	2.02	0.20	0.13	0.12	2.82	0.64	0.01	0.00
38	0.03	0.01	0.01	0.01	0.02	0.01	0.03	0.02	0.03	0.00
45	0.66	0.19	8.84	2.84	0.72	0.47	30.10	4.01	0.03	0.00

**Table A3.** Results of dust emission measurements performed at velocity  $v_2 = 15.5$  m/s.

Day	Biopolymer						ControlC	
	CS		FBPC		XG		M	SD
	M	SD	M	SD	M	SD		
TSPs (mg/m <sup>3</sup> )								
2	0.22	0.20	0.27	0.12	0.07	0.04	39.20	16.19
8	0.09	0.02	0.09	0.01	0.11	0.02	5.45	1.72
15	1.25	0.58	13.50	2.33	2.77	1.04	24.83	3.62
25	31.07	2.89	14.47	1.58	19.83	3.73	39.07	23.39
32	0.55	0.23	2.46	1.25	0.19	0.12	8.27	5.11
38	0.12	0.06	0.02	0.01	0.01	0.00	0.00	0.00
45	0.59	0.17	13.67	5.54	1.10	0.55	21.13	4.83
PM <sub>10</sub> (mg/m <sup>3</sup> )								
2	0.15	0.14	0.18	0.08	0.05	0.03	38.40	16.01
8	0.08	0.02	0.07	0.01	0.09	0.02	4.09	1.29
15	1.25	0.58	13.00	2.33	2.61	0.92	24.37	3.58
25	30.20	2.73	13.73	1.65	19.10	3.68	38.23	23.15
32	0.49	0.22	2.35	1.20	0.18	0.11	7.99	5.11
38	0.10	0.05	0.02	0.01	0.01	0.00	0.00	0.00
45	0.54	0.15	13.38	5.46	1.04	0.53	20.80	4.81
PM <sub>2.5</sub> (mg/m <sup>3</sup> )								
2	0.05	0.04	0.09	0.05	0.03	0.01	37.43	15.80
8	0.06	0.02	0.05	0.00	0.06	0.02	2.23	0.71
15	1.25	0.58	12.59	2.29	2.47	0.83	24.07	3.50
25	29.57	2.58	13.00	1.85	18.77	3.63	37.58	22.96
32	0.46	0.22	2.28	1.19	0.16	0.11	7.79	5.13
38	0.09	0.04	0.02	0.01	0.01	0.00	0.00	0.00
45	0.51	0.15	13.19	5.39	0.98	0.51	20.53	4.76

**Table A4.** Results of dust emission measurements performed at velocity  $v_3 = 17.4$  m/s.

Day	Biopolymer						ControlC	
	CS		FBPC		XG		M	SD
	M	SD	M	SD	M	SD		
TSPs (mg/m <sup>3</sup> )								
2	0.06	0.01	0.22	0.05	0.05	0.02	22.83	10.04
8	0.08	0.01	0.12	0.03	0.12	0.04	7.16	1.43
15	1.10	0.52	7.42	1.74	64.00	11.87	12.20	10.48
25	25.33	7.67	14.43	1.54	37.73	5.28	39.20	2.36
32	0.55	0.33	2.46	0.91	0.20	0.16	4.48	5.14
38	0.08	0.00	0.01	0.00	0.02	0.00	0.04	0.02
45	0.86	0.40	8.93	2.80	5.50	1.79	28.23	3.51
PM <sub>10</sub> (mg/m <sup>3</sup> )								
2	0.05	0.01	0.16	0.04	0.04	0.01	22.13	9.97
8	0.07	0.00	0.10	0.02	0.10	0.03	5.74	1.20
15	1.10	0.52	6.75	2.11	62.83	11.65	11.97	10.22
25	24.90	7.43	13.87	1.44	36.80	5.27	37.83	2.27
32	0.50	0.31	2.31	0.84	0.17	0.13	4.34	4.95
38	0.06	0.00	0.01	0.00	0.02	0.00	0.04	0.02
45	0.81	0.38	8.81	2.79	5.30	1.74	27.83	3.59
PM <sub>2.5</sub> (mg/m <sup>3</sup> )								
2	0.02	0.01	0.08	0.03	0.02	0.00	21.37	9.86
8	0.04	0.00	0.07	0.01	0.07	0.02	3.69	0.81
15	1.10	0.52	5.90	2.82	61.93	11.56	11.77	10.01
25	24.57	7.27	13.50	1.39	36.17	5.15	36.57	2.18
32	0.48	0.30	2.20	0.78	0.15	0.12	4.30	4.91
38	0.05	0.01	0.01	0.00	0.02	0.00	0.04	0.02
45	0.77	0.39	8.71	2.78	5.15	1.69	27.43	3.66

**Table A5.** Results of the penetrometer tests conducted on the trial areas treated with CS, FBPC, XG and the untreated control area. Tests were performed with twenty replicates ( $n = 20$ ).

Day	Biopolymer						Control	
	CS		FBPC		XG		C	
	M	SD	M	SD	M	SD	M	SD
Penetration Resistance (N)								
2	20.26	13.59	17.56	11.93	8.63	5.05	3.63	8.87
8	19.23	5.62	18.88	5.82	6.67	6.37	3.58	4.31
15	2.11	1.36	9.81	5.90	4.71	2.97	3.24	3.84
25	2.84	0.98	8.98	4.35	3.04	1.45	5.20	1.78
32	4.76	1.40	8.73	2.48	5.05	1.25	4.46	1.33
38	7.31	2.60	8.24	3.60	5.35	2.43	6.72	2.91
45	8.49	3.71	6.62	3.02	6.18	4.00	5.20	6.04

Note. M = Mean, SD = Standard deviation.

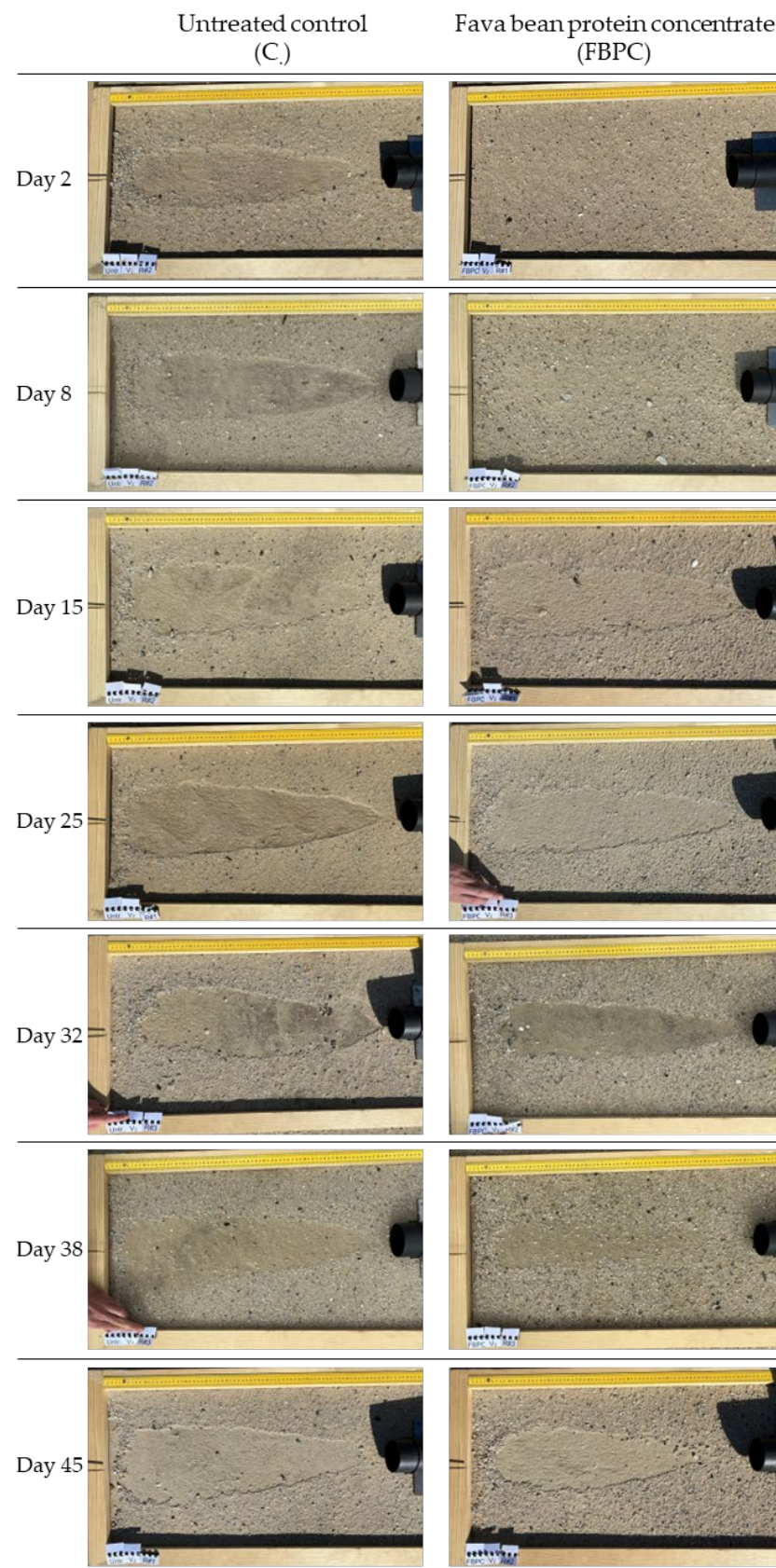


**Figure A1.** Exemplary photographs of untreated control (C) and FBPC-treated trial plots after subjecting them to air speed of  $v_2$  (15.5 m/s) for 60 s. The trial plots had dimensions of  $40 \times 70 \text{ cm}^2$ .

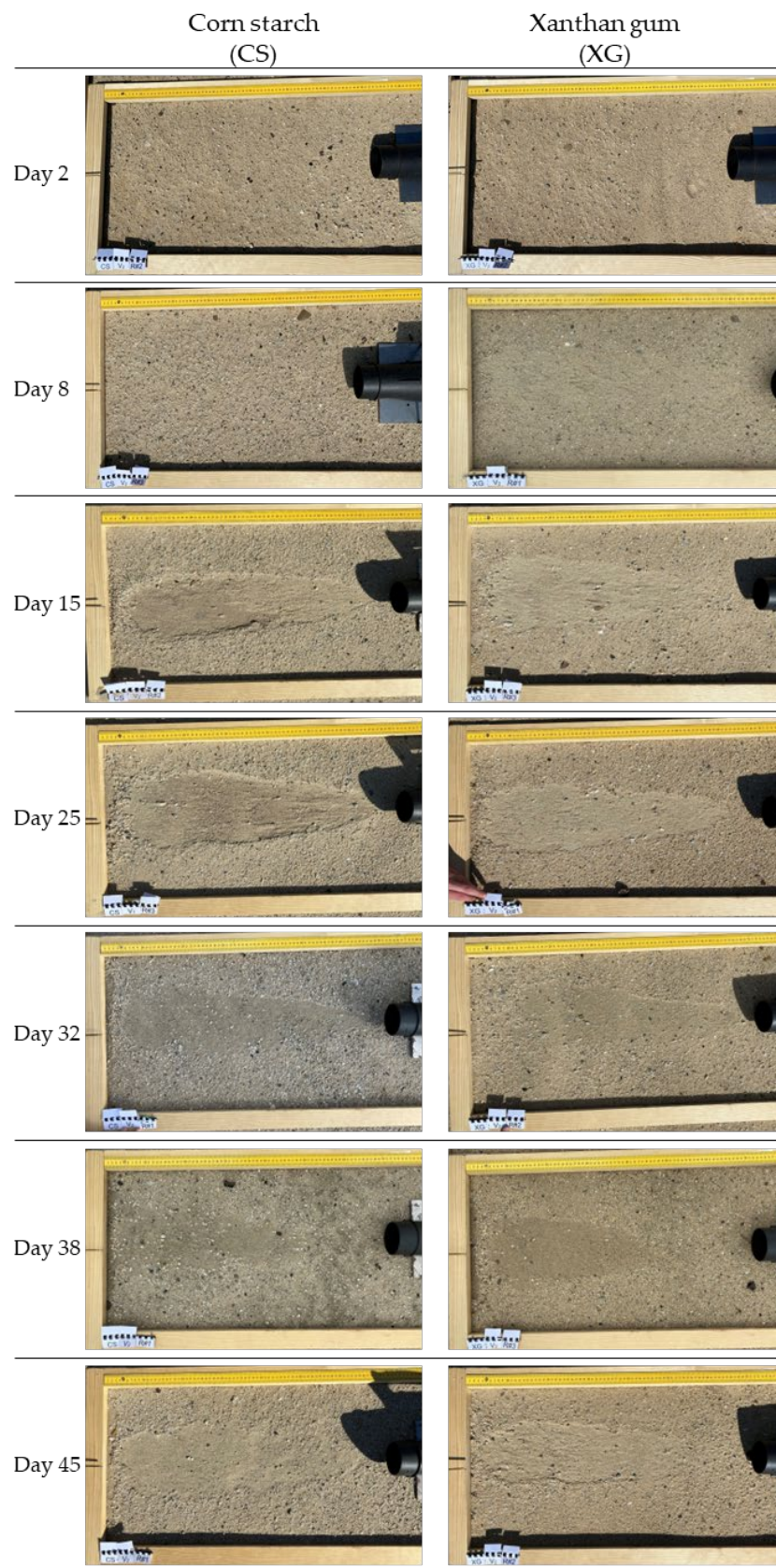


**Figure A2.** Exemplary photographs of CS- and XG-treated trial plots after subjecting them to air speed of  $v_2$  (15.5 m/s) for 60 s. The trial plots had dimensions of  $40 \times 70 \text{ cm}^2$ .



**Figure A3.** Exemplary photographs of untreated control (C) and FBPC-treated trial plots after subjecting them to air speed of  $v_3$  (17.4 m/s) for 60 s. The trial plots had dimensions of  $40 \times 70 \text{ cm}^2$ .

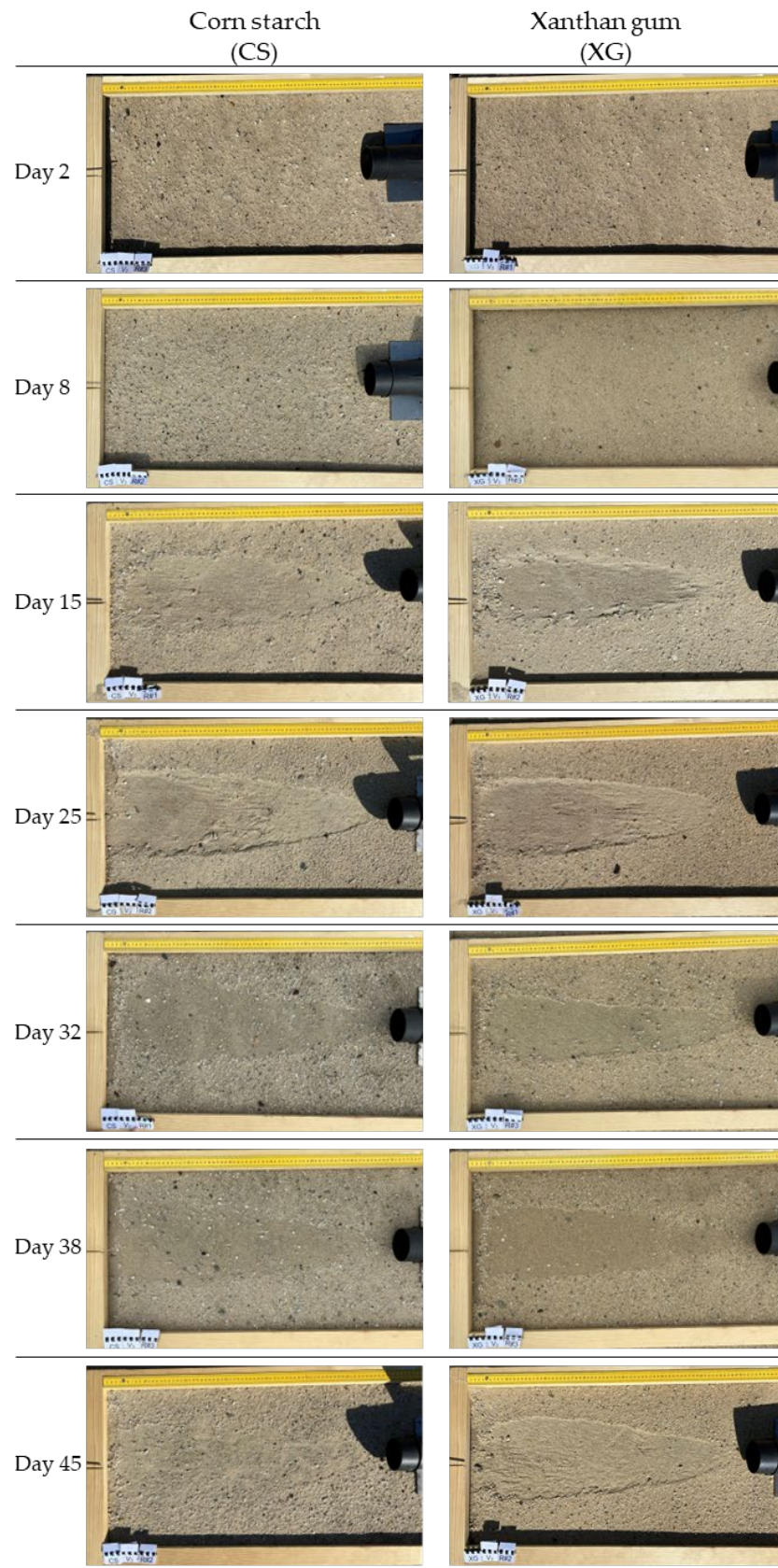


**Figure A4.** Exemplary photographs of CS- and XG-treated trial plots after subjecting them to air speed of  $v_3$  (17.4 m/s) for 60 s. The trial plots had dimensions of  $40 \times 70 \text{ cm}^2$ .

**Table A6.** Compilation of previous field trials testing the application of dust suppressants on exposed, undisturbed soils.

Substances	C (%)	AR (L/m <sup>2</sup> )	Test Field	Dur.	Conclusion	Note	Ref
Dust Fyghter (pulp proc. by-product)	25.0	0.8	Soil: Tailings Site: TSF Size: 2.5 × 16 m <sup>2</sup>	4 m	<ul style="list-style-type: none"> <li>Averaged over study, the mean emission rates of all test plots (incl. suppressants and control) were similar high and showed high variability.</li> </ul>	a, b, c, e	[55]
Entac (pulp proc. by-product)	20.0	1.4				a, b, d	[55]
EcoAnchor (acrylic polymer)	11.0	10.0				a, b, c	[55]
Soil Sement (acrylic polymer)	10.0	1.0				a, b, c	[55]
Tall oil pitch	20.0	2.0	Soil: Sandy loam Size: 16 × 16 m <sup>2</sup>	14 m	<ul style="list-style-type: none"> <li>Significant reduction in PM10 emissions for first 3–6 months</li> </ul>	c	[56]
	17.0	2.0				c	[56]
	14.0	2.0				c	[56]
Chicory vinasses	10.0	1.5	Soil: SP Size: 0.4 × 0.7 m <sup>2</sup>	1 m	<ul style="list-style-type: none"> <li>Considerable short-term reduction in dust emissions until D14</li> <li>Rainfall as main impairing factor</li> </ul>	c, e	[47]
Corn steep liquor	5.0	0.8				c, e	[47]
Decantation syrup	6.0	1.0				c, e	[47]
Palatinose molasses	6.0	1.0				c, e	[47]
Poloxamer	5.6	N/A	Soil: Tailings Site: TSF beach Size: N/A	2 w	<ul style="list-style-type: none"> <li>TSF beach: Reduction in PM10 by 50% in week 1, and almost no effect in week 2</li> <li>TSF slope: Reduction in PM10 by 73% in week 1, and almost no effect in week 2</li> </ul>	c, e	[54]
Poloxamer	5.6	18.5	Soil: Tailings Site: TSF slope Size: 36 × 6 m <sup>2</sup>		<ul style="list-style-type: none"> <li>Rainfall likely main impairing factor</li> <li>Moisture retention main mechanism</li> </ul>	c, e	[54]
Starch + polyacrylamide (10:1)	0.7, 1.0, 1.3	5 × 0.67 kg/m <sup>2</sup>	Soil: Loess Size: N/A	1 m	<ul style="list-style-type: none"> <li>One-month effective dust suppression</li> <li>Aggregation and crust formation as main mechanisms</li> </ul>	c, d, e	[57]

Note. AR = application rate, C = concentration, Dur = duration, m = month, N/A = not available, Ref = reference, TSF = tailings storage facility, w = week, a = product dosage (dry matter of substance unknown), b = deliberately induced physical disturbance by skid steer track after third test day, c = substance applied by a single application, d = substance applied in 3 coats, each 20 min apart, e = application regime not clearly explained in the source. It is assumed that the suppressant was applied over five days, each day at 0.67 kg/m<sup>2</sup>, e = tests performed with portable in situ soil wind erosion laboratory (PI-SWERL).

## References

- Neitlich, P.N.; Berryman, S.; Geiser, L.H.; Mines, A.; Shiel, A.E. Impacts on tundra vegetation from heavy metal-enriched fugitive dust on National Park Service lands along the Red Dog Mine haul road, Alaska. *PLoS ONE* **2022**, *17*, e0269801. [[CrossRef](#)] [[PubMed](#)]
- Ekpa, I.D.; Laniyan, D.G.; Agbor, C.N.; Ben, U.C.; Okon, J.E. Effect of air pollution from quarry activities on agriculture and plant biodiversity in South-Eastern Nigeria. *Res. Sq.* **2022**. [[CrossRef](#)]
- Noble, T.L.; Parbhakar-Fox, A.; Berry, R.F.; Lottermoser, B. Mineral dust emissions at metalliferous mine sites. In *Environmental Indicators in Metal Mining*; Lottermoser, B., Ed.; Springer International Publishing: Cham, Switzerland, 2016; pp. 281–306; ISBN 978-3-319-42729-4.
- Entwistle, J.A.; Hursthouse, A.S.; Marinho Reis, P.A.; Stewart, A.G. Metalliferous mine dust: Human health impacts and the potential determinants of disease in mining communities. *Curr. Pollut. Rep.* **2019**, *5*, 67–83. [[CrossRef](#)]
- Cecala, A.B.; O'Brien, A.D.; Schall, J.; Colinet, J.F.; Franta, R.J.; Schultz, M.J.; Haas, E.J.; Robinson, J.E.; Patts, J.; Holen, B.M.; et al. *Dust Control Handbook for Industrial Minerals Mining and Processing*, 2nd ed.; U.S. Department of Health and Human Services, Public Health Service, Centers for Disease Control and Prevention, National Institute for Occupational Safety and Health: Pittsburgh, PA, USA, 2019.
- Iyaloo, S.; Kootbodien, T.; Naicker, N.; Mathee, A.; Kgalamono, S.; Wilson, K.; Rees, D. O3A.5 Environmental dust exposure from gold mine waste dumps and respiratory health effects in Johannesburg, South Africa. *Occup. Environ. Med.* **2019**, *76*, 22–23. [[CrossRef](#)]
- Zota, A.R.; Riederer, A.M.; Ettinger, A.S.; Schaidler, L.A.; Shine, J.P.; Amarasiriwardena, C.J.; Wright, R.O.; Spengler, J.D. Associations between metals in residential environmental media and exposure biomarkers over time in infants living near a mining-impacted site. *J. Expo. Sci. Environ. Epidemiol.* **2016**, *26*, 510–519. [[CrossRef](#)] [[PubMed](#)]
- Boreland, F.; Lyle, D.M. Lead dust in Broken Hill homes: Effect of remediation on indoor lead levels. *Environ. Res.* **2006**, *100*, 276–283. [[CrossRef](#)]
- Barbieri, E.; Fontúrbel, F.E.; Herbas, C.; Barbieri, F.L.; Gardon, J. Indoor metallic pollution and children exposure in a mining city. *Sci. Total Environ.* **2014**, *487*, 13–19. [[CrossRef](#)]

10. Thompson, R.J.; Visser, A.T. Selection, performance and economic evaluation of dust palliatives on surface mine haul roads. *J. S. Afr. Inst. Min. Metall.* **2007**, *107*, 435–450.
11. du Plessis, J.J.; Jansen van Rensburg, L. Effectiveness of applying dust suppression palliatives on haul roads. *J. Mine Vent. Soc. S. Afr.* **2015**, *69*, 15–19.
12. Clarke, B.; Otto, F.; Stuart-Smith, R.; Harrington, L. Extreme weather impacts of climate change: An attribution perspective. *Environ. Res. Clim.* **2022**, *1*, 12001. [[CrossRef](#)]
13. IPCC. *Climate Change 2022: Impacts, Adaptation and Vulnerability: Contribution of Working Group II to the Sixth Assessment Report of the Intergovernmental Panel on Climate Change 2022*; Cambridge University Press: Singapore, 2022. [[CrossRef](#)]
14. OECD. *Global Material Resources Outlook to 2060: Economic Drivers and Environmental Consequences*; OECD Publishing: Paris, France, 2019; ISBN 9789264307445.
15. Piechota, T.; van Ee, J.; Stave, K.; James, D. *Potential Environmental Impacts of Dust Suppressants: "Avoiding Another Times Beach"*; U.S. Environmental Protection Agency: Las Vegas, NV, USA, 2002.
16. McTigue, E.; Zimmermann, J.H.; Duncan, B.; Bertelsen, L.; Gavrelis, N.; Deng, M. *Research Findings: Data Collection on Toxicity of Dust Palliatives Used in Alaska*; U.S. Environmental Protection Agency: Washington, DC, USA, 2016. Available online: [https://cfpub.epa.gov/si/si\\_public\\_record\\_report.cfm?dirEntryId=328330&Lab=NERL](https://cfpub.epa.gov/si/si_public_record_report.cfm?dirEntryId=328330&Lab=NERL) (accessed on 11 June 2023).
17. IEA—International Energy Agency. *The Future of Petrochemicals*; International Energy Agency: Paris, France, 2018. Available online: [https://iea.blob.core.windows.net/assets/bee4ef3a-8876-4566-98cf-7a130c013805/The\\_Future\\_of\\_Petrochemicals.pdf](https://iea.blob.core.windows.net/assets/bee4ef3a-8876-4566-98cf-7a130c013805/The_Future_of_Petrochemicals.pdf) (accessed on 11 June 2023).
18. Dagliya, M.; Satyam, N.; Garg, A. Biopolymer based stabilization of Indian desert soil against wind-induced erosion. *Acta Geophys.* **2023**, *71*, 503–516. [[CrossRef](#)]
19. Lemboye, K.; Almajed, A.; Alnuaim, A.; Arab, M.; Alshibli, K. Improving sand wind erosion resistance using renewable agriculturally derived biopolymers. *Aeolian Res.* **2021**, *49*, 100663. [[CrossRef](#)]
20. Owji, R.; Habibagahi, G.; Nikooee, E.; Afzali, S.F. Wind erosion control using carboxymethyl cellulose: From sand bombardment performance to microfabric analysis. *Aeolian Res.* **2021**, *50*, 100696. [[CrossRef](#)]
21. Toufigh, V.; Ghassemi, P. Control and stabilization of fugitive dust: Using eco-friendly and sustainable materials. *Int. J. Geomech.* **2020**, *20*, 4020140. [[CrossRef](#)]
22. Phillips, G.O.; Edwards, C.A.; Garcia, A.L.; Williams, P.A.; Dickinson, E.; Armisen, R.; Taggart, P.; Mitchell, J.R.; Haug, I.J.; Draget, K.I.; et al. *Handbook of Hydrocolloids*, 2nd ed.; CRC/Woodhead: Boca Raton, FL, USA; Oxford, UK, 2009; ISBN 978-1-84569-414-2.
23. Chaturvedi, S.; Kulshrestha, S.; Bhardwaj, K.; Jangir, R. A review on properties and applications of xanthan gum. In *Microbial Polymers*; Vaishnav, A., Choudhary, D.K., Eds.; Springer: Singapore, 2021; pp. 87–107; ISBN 978-981-16-0044-9.
24. Ding, X.; Xu, G.; Zhang, Y.; Luo, Z.; Deng, J. Reduction of airborne bauxite residue dust pollution by enhancing the structural stability via the application of non-traditional stabilizers. *Water Air Soil Pollut.* **2021**, *232*, 1–20. [[CrossRef](#)]
25. Ding, X.; Luo, Z.; Xu, G.; Chang, P. Characterization of red sand dust pollution control performance via static and dynamic laboratorial experiments when applying polymer stabilizers. *Environ. Sci. Pollut. Res. Int.* **2021**, *28*, 34937–34952. [[CrossRef](#)]
26. Almajed, A.; Lemboye, K.; Arab, M.G.; Alnuaim, A. Mitigating wind erosion of sand using biopolymer-assisted EICP technique. *Soils Found.* **2020**, *60*, 356–371. [[CrossRef](#)]
27. Ding, X.; Xu, G.; Zhou, W.; Kuruppu, M. Effect of synthetic and natural polymers on reducing bauxite residue dust pollution. *Environ. Technol.* **2018**, *41*, 1–10. [[CrossRef](#)]
28. Ding, X.; Xu, G.; Kizil, M.; Zhou, W.; Guo, X. Lignosulfonate treating bauxite residue dust pollution: Enhancement of mechanical properties and wind erosion behavior. *Water Air Soil Pollut.* **2018**, *229*, 1084. [[CrossRef](#)]
29. Hu, Y.; Shi, L.; Shan, Z.; Dai, R.; Chen, H. Efficient removal of atmospheric dust by a suppressant made of potato starch, polyacrylic acid and gelatin. *Environ. Chem. Lett.* **2020**, *18*, 1701–1711. [[CrossRef](#)]
30. Chen, R.; Lee, I.; Zhang, L. Biopolymer stabilization of mine tailings for dust control. *J. Geotech. Geoenviron. Eng.* **2014**, *141*, 4014100. [[CrossRef](#)]
31. Tran, T.P.A.; Cho, G.-C.; Ilhan, C. Water retention characteristics of biopolymer hydrogel-treated sand-clay mixture. *HueUni-JESE* **2020**, *129*, 5–17. [[CrossRef](#)]
32. Katra, I. Comparison of diverse dust control products in wind-induced dust emission from unpaved roads. *Appl. Sci.* **2019**, *9*, 5204. [[CrossRef](#)]
33. Kavazanjian, E.; Iglesias, E.; Karatas, I. Biopolymer soil stabilization for wind erosion control. In Proceedings of the 17th International Conference on Soil Mechanics and Geotechnical Engineering, Alexandria, Egypt, 5–9 October 2009; Hamza, M., Shahien, M., El-Mossallamy, Y., Eds.; IOS Press: Amsterdam, The Netherlands, 2009. ISBN 978-1-60750-031-5.
34. Ayeldeen, M.; Negm, A.; El Sawwaf, M.; Gädä, T. Laboratory study of using biopolymer to reduce wind erosion. *Int. J. Geo-Eng.* **2017**, *12*, 228–240. [[CrossRef](#)]
35. Chang, I.; Lee, M.; Tran, A.T.P.; Lee, S.; Kwon, Y.-M.; Im, J.; Cho, G.-C. Review on biopolymer-based soil treatment (BPST) technology in geotechnical engineering practices. *Transportation Geotechnics. Transp. Geotech.* **2020**, *24*, 100385. [[CrossRef](#)]
36. Wade, E.; Zowada, R.; Foudazi, R. Alginate and guar gum spray application for improving soil aggregation and soil crust integrity. *Carbohydr. Polym.* **2021**, *2*, 100114. [[CrossRef](#)]
37. Sieger, J.L.; Lottermoser, B.G.; Freer, J. Evaluation of protein and polysaccharide biopolymers as dust suppressants on mine soils: Laboratory experiments. *Appl. Sci.* **2023**, *13*, 1010. [[CrossRef](#)]

38. Sieger, J.L.; Lottermoser, B.G.; Freer, J. Effectiveness of protein and polysaccharide biopolymers as dust suppressants on mine soils: Results from wind tunnel and penetrometer testing. *Appl. Sci.* **2023**, *13*, 4158. [CrossRef]
39. DIN EN ISO 17892-4; Geotechnical Investigation and Testing—Laboratory Testing of Soil—Part 4: Determination of Particle Size Distribution. German Institute for Standardization: Berlin, Germany, 2017.
40. Google Maps. *Tagebau Inden Open Pit Mine*; Google Maps: Mountain View, CA, USA, 2022.
41. AST D2487-17; Standard Practice for Classification of Soils for Engineering Purposes (Unified Soil Classification System). ASTM International: West Conshohocken, PA, USA, 2018.
42. DIN EN ISO 11508:2017; Soil Quality—Determination of Particle Density. German Institute for Standardization: Berlin, Germany, 2018.
43. DIN EN 15933:2012-11; Sludge, Treated Biowaste and Soil—Determination of pH. German Institute for Standardization: Berlin, Germany, 2012.
44. ISO 10625; Equipment for Crop Protection—Sprayer Nozzles—Colour Coding for Identification. ISO: Geneva, Switzerland, 2018.
45. WHO. *WHO Global Air Quality Guidelines: Particulate Matter (PM<sub>2.5</sub> and PM<sub>10</sub>), Ozone, Nitrogen Dioxide, Sulfur Dioxide and Carbon Monoxide*; WHO European Centre for Environment and Health: Bonn, Germany, 2021; ISBN 9789240034228.
46. ISO 12103-1; Road Vehicles—Test Contaminants for Filter Evaluation: Part 1: Arizona Test Dust. ISO: Geneva, Switzerland, 2023.
47. Freer, J.; Lübeck, M.; Sieger, J.L.; Lottermoser, B.G.; Braun, M. Effectiveness of food processing by-products as dust suppressants for exposed mine soils: Results from laboratory experiments and field trials. *Appl. Sci.* **2022**, *12*, 11551. [CrossRef]
48. van Pelt, R.S.; Zobeck, T.M. Portable wind tunnels for field testing of soils and natural surfaces. In *Wind Tunnel Designs and Their Diverse Engineering Applications*; Ahmed, N., Ed.; InTech: London, UK, 2013; ISBN 978-953-51-1047-7.
49. Gotosa, J.; Nyamadzawo, G.; Mtetwa, T.; Kanda, A.; Dudu, V. Comparative road dust suppression capacity of molasses stillage and water on gravel road in Zimbabwe. *AIR* **2015**, *3*, 198–208. [CrossRef]
50. Gillies, J.A.; Watson, J.G.; Rogers, C.F.; DuBois, D.; Chow, J.C.; Langston, R.; Sweet, J. Long-term efficiencies of dust suppressants to reduce PM<sub>10</sub> emissions from unpaved roads. *J. Air Waste Manag. Assoc.* **1999**, *49*, 3–16. [CrossRef] [PubMed]
51. Parsakhoo, A.; Hosseini, S.A.; Lotfalian, M.; Mohammadi, J.; Salarijazi, M. Effects of molasses, polyacrylamide and bentonite on dust control in forest roads. *J. For. Sci.* **2020**, *66*, 218–225. [CrossRef]
52. Omane, D.; Liu, W.V.; Pourrahimian, Y. Comparison of chemical suppressants under different atmospheric temperatures for the control of fugitive dust emission on mine hauls roads. *Atmos. Pollut. Res.* **2018**, *9*, 561–568. [CrossRef]
53. Edvardsson, K.; Gustafsson, A.; Magnusson, R. Dust suppressants efficiency study: In situ measurements of dust generation on gravel roads. *Int. J. Pavement Eng.* **2012**, *13*, 11–31. [CrossRef]
54. Park, J.; Kim, K.; Lee, T.; Kim, M. Tailings storage facilities (TSFs) dust control using biocompatible polymers. *Min. Metall. Explor.* **2019**, *36*, 785–795. [CrossRef]
55. Preston, C.A.; McKenna Neuman, C.; Boulton, J.W. A wind tunnel and field evaluation of various dust suppressants. *J. Air Waste Manag. Assoc.* **2020**, *70*, 915–931. [CrossRef] [PubMed]
56. Kavouras, I.G.; Etyemezian, V.; Nikolich, G.; Gillies, J.; Sweeney, M.; Young, M.; Shafer, D. A new technique for characterizing the efficacy of fugitive dust suppressants. *J. Air Waste Manag. Assoc.* **2009**, *59*, 603–612. [CrossRef]
57. Shen, Z.; Ao, Z.; Wang, Z.; Yang, Y. Study on crust-shaped dust suppressant in non-disturbance area of open-pit coal mine—A case study. *Int. J. Environ. Res. Public Health* **2023**, *20*, 934. [CrossRef]
58. Jones, D. *Guidelines for the Selection, Specification and Application of Chemical Dust Control and Stabilization Treatments on Unpaved Roads*; University of California Pavement Research Center: Davis, CA, USA, 2017. Available online: <http://www.ucprc.ucdavis.edu/PDF/UCPRC-GL-2017-03.pdf> (accessed on 11 June 2023).
59. Fatehi, H.; Ong, D.E.L.; Yu, J.; Chang, I. Biopolymers as green binders for soil improvement in geotechnical applications: A review. *Geosci. J.* **2021**, *11*, 291. [CrossRef]
60. Mendonça, A.; Morais, P.V.; Pires, A.C.; Chung, A.P.; Oliveira, P.V. A Review on the importance of microbial biopolymers such as xanthan gum to improve soil properties. *Appl. Sci.* **2021**, *11*, 170. [CrossRef]
61. Bacon, S.N.; McDonald, E.V.; Amit, R.; Enzel, Y.; Crouvi, O. Total suspended particulate matter emissions at high friction velocities from desert landforms. *J. Geophys. Res.* **2011**, *116*, 1–17. [CrossRef]
62. King, J.; Etyemezian, V.; Sweeney, M.; Buck, B.J.; Nikolich, G. Dust emission variability at the Salton Sea, California, USA. *Aeolian Res.* **2011**, *3*, 67–79. [CrossRef]
63. Chen, R.; Ding, X.; Ramey, D.; Lee, I.; Zhang, L. Experimental and numerical investigation into surface strength of mine tailings after biopolymer stabilization. *Acta Geotech.* **2016**, *11*, 1075–1085. [CrossRef]
64. Thomas, A.D.; Dougill, A.J. Spatial and temporal distribution of cyanobacterial soil crusts in the Kalahari: Implications for soil surface properties. *Geomorphology* **2007**, *85*, 17–29. [CrossRef]
65. Pérez, F.L. Microbiotic crusts in the high equatorial Andes, and their influence on paramo soils. *CATENA* **1997**, *31*, 173–198. [CrossRef]
66. Zaady, E.; Ben-David, E.A.; Sher, Y.; Tzirkin, R.; Nejidat, A. Inferring biological soil crust successional stage using combined PLFA, DGGE, physical and biophysiological analyses. *Soil Biol. Biochem.* **2010**, *42*, 842–849. [CrossRef]
67. Li, J.; Okin, G.S.; Herrick, J.E.; Belnap, J.; Munson, S.M.; Miller, M.E. A simple method to estimate threshold friction velocity of wind erosion in the field. *Geophys. Res. Lett.* **2010**, *37*, 1–5. [CrossRef]

68. Houser, C.A.; Nickling, W.G. The factors influencing the abrasion efficiency of saltating grains on a clay-crusting playa. *Earth Surf. Process. Landf.* **2001**, *26*, 491–505. [[CrossRef](#)]
69. Swet, N.; Kutra, I. Reduction in soil aggregation in response to dust emission processes. *Geomorphology* **2016**, *268*, 177–183. [[CrossRef](#)]
70. Sweeney, M.; Etyemezian, V.; Macpherson, T.; Nickling, W.; Gillies, J.; Nikolich, G.; McDonald, E. Comparison of PI-SWRL with dust emission measurements from a straight-line field wind tunnel. *J. Geophys. Res.* **2008**, *113*, 1–12. [[CrossRef](#)]
71. Jang, J. A review of the application of biopolymers on geotechnical engineering and the strengthening mechanisms between typical biopolymers and soils. *Adv. Mater. Sci. Eng.* **2020**, *2020*, 1–20. [[CrossRef](#)]
72. Heusala, H.; Sinkko, T.; Sözer, N.; Hytönen, E.; Mogensen, L.; Knudsen, M.T. Carbon footprint and land use of oat and faba bean protein concentrates using a life cycle assessment approach. *J. Clean. Prod.* **2020**, *242*, 118376. [[CrossRef](#)]
73. Steevens, J.; Suedel, B.; Gibson, A.; Kennedy, A.; Blackburn, W.; Splichal, D.; Pierce, T. Environmental Evaluation of Dust Stabilizer Products. Available online: <https://apps.dtic.mil/sti/pdfs/ADA471771.pdf> (accessed on 11 June 2023).

**Disclaimer/Publisher’s Note:** The statements, opinions and data contained in all publications are solely those of the individual author(s) and contributor(s) and not of MDPI and/or the editor(s). MDPI and/or the editor(s) disclaim responsibility for any injury to people or property resulting from any ideas, methods, instructions or products referred to in the content.